END EFFECTOR RESPONSE AND STABILITY OF A ROBOTIC MANIPULATOR UNDER DETERMINISTIC AND RANDOM BASE – EXCITATION

by

Ashim Roy

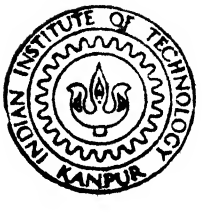

DEPARTMENT OF MECHANICAL ENGINEERING

INDIAN INSTITUTE OF TECHNOLOGY KANPUR

FEBRUARY, 1992

END EFFECTOR RESPONSE AND STABILITY OF A ROBOTIC MANIPULATOR UNDER DETERMINISTIC AND RANDOM BASE-EXCITATION

A Thesis submitted

In Partial fulfilment Of the Requirements

For the Degree of

MASTER OF TECHNOLOGY

by

ASHIM ROY

to the

DEPARTMENT OF MECHANICAL ENGINEERING

INDIAN INSTITUTE OF TECHNOLOGY KANPUR

FEBRUARY, 1992

ME-1992-M-ROY-END

ACKNOWLEDGEMENTS

I am deeply grateful to Dr. B. Sahay for his contin guidance, patience and encouragement during the entire duration my research. His infectious enthusiasm and his ready availabil to advise me with work are very much appreciated.

I would like to thank I.I.T, Kanpur for the first cl education offered to me. I offer my heartfelt thanks to my frie who gave me a constant charge of inspiration for a bet completion of my work. Finally, I dedicate my thesis to my pare who gave up their dreams so that I could have mine and for this shall remain forever in their debt.

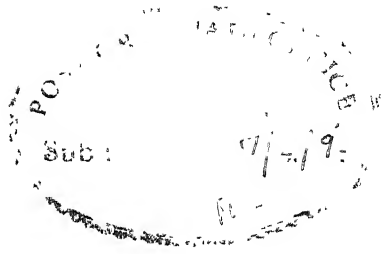

CERTIFICATE

It is certified that the present work entitled *"END EFFECTOR RESPONSE AND STABILITY OF A ROBOTIC MANIPULATOR UNDER DETERMINISTIC AND RANDOM BASE-EXCITATION"* has been carried out by Mr. ASHIM ROY under my supervision and that it has not been submitted elsewhere for a degree.

FEBRUARY, 1002

(Dr. B.SAHAY)

Professor

Department of mechanical Engineering

Indian Institute of Technology, Kanpur

NOMENCLATURE

θ_n	Rotation of n^{th} joint with respect to Z_{n-1} axis.
ϕ_n	Angle made by the n^{th} link with the horizontal.
M_n, L_n, R_n	Mass, length and radius of n^{th} link.
$\left[{}^{i}_{i-1}T\right]$	Transformation matrix between $(i-1)^{th}$ and i^{th} frames.
[Trans(a,b,c)]	Translation by 'a' along 'X' axis, 'b' along 'Y' axis and 'c' along 'Z' axis.
Rot(axis1,θ)	Rotation of any link by an angle 'θ' about the axis 'axis1'.
$\left[{}^{i}I_{xx}\right]$	Moment of inertia of the i^{th} link about its own 'x' axis.
$\left[{}^{i}I_{yy}\right]$	Moment of inertia of the i^{th} link about its own 'y' axis.
$\left[{}^{i}I_{zz}\right]$	Moment of inertia of the i^{th} link about its own 'z' axis.
K_n	Joint stiffness of n^{th} link.
Q	Generalized force.
ω	Frequency of forcing function.
ω_n	natural frequency of the system.
ξ	Damping factor.
C_o, C_1	Damping parameters.
S_p	Spectral density of excitation.

TABLE OF CONTENTS

LIST OF TABLES AND FIGURES

PAGE

ABSTRACT

The stability and response of the end effector of a 2_D.O.F as well as five and six D.O.F manipulators subject to base excitation is investigated. The manipulators consist of rigid links that are connected end-to-end in an open chain. The connections between the base and the first link and between two successive links are characterized by resilient joints. Due to this compliance in its joints, the manipulator undergoes oscillatory motions when perturbed from its equilibrium configuration. The end effector is assumed to carry a load at its free extremity. When the intensity of this load reaches some critical value, the manipulator becomes unstable by divergence. The numerical values of the critical divergence load for various configurations of the manipulator are computed. The weakest configuration of the manipulator when the critical divergence load is the minimum is also found out. The behavior of the response of the end effector subject to deterministic and probabilistic excitations have been investigated. Finally, a comparison has been made amongst different D.O.F manipulators when a white noise of constant spectral density acts at the bases.

CHAPTER 1

INTRODUCTION

1.1 Preface

Robot, in general, is an automatic, reprogrammable, multifunctional,mechanical manipulator. Ideally, without any human intervention, it can work independently using its own machine intelligence. It works more precisely than human being with higher repeatability and virtually no exhaustion. It can perform tasks such as assembly of electrical, electronics and mechanical parts eg. PCB, miniature ball bearings etc., peg-hole insertion, telechiric operations, welding of micro parts, spray paintings etc.. All these operations require accuracy of the order of 0.1 to 0.01 mm. Hence the precision of such type of robots is of utmost importance .

One of the main areas of robotic development today concentrates itself on the control of positional accuracy. The controller of a robot regulates the mechanical positioning of the end effector within the least amount of inaccuracy. This inaccuracy is not completely avoidable and is caused primarily due to joint compliance, link flexibility and incapability of the controller to operate upon data extending to several places of

decimals. In recent times, there is a tendency to develop light weight robots which have the obvious advantage of lower space requirements, greater mobility and higher operating speed. For example, CANADA-ARM which is used in space for retrieving artificial satellites for repairs and then putting them back into the parking orbit, is a light-weight long flexible telechiric robot. This structure has compliance in joints and links due to the reduction in cross-sections. While in operation, it undergoes some motion-induced vibrations which has to be damped out as quickly as possible so that the end effector can perform its tasks with less inaccuracy. When the mass of the load exceeds the mass of the manipulator, the elasticity in the links can become of considerable importance, as has been reported by Sunada and Dubowsky [1]. Moreover, if the environment in which the robot works is not free from vibration coming from other machineries, or in the case of mobile robots, where floor surface is not devoid of roughness and undulations, the positional inaccuracy can go up. Hence, a thorough understanding and quantitative analysis of the response characteristics of the end effector tip of the manipulator is required .

1.2 FACTORS AFFECTING ACCURACY

The positioning accuracy and repeatability of a robot depends on some factors such as [10] given below.

1> The force of gravity acting on the arm members and load of the robot causes downward deflection of the arm and the support

system. This is referred to as joint and link flexibility .

2> Acceleration forces may act in various directions. Noticeable horizontal and vertical deflections occur when heavy loads are accelerated .

3>Drive gears and belt drives often have noticeable amount of slack that can cause positioning errors.

4> Thermal effects can expand or contract the links of the robot. In large robots, this effect can be of considerable magnitude.

5> Bearing "PLAY" can be significant when very high positioning accuracies are required .

5> Low resolution of the controller,in some cases may also be responsible for poor accuracy.

6> The feedback errors arising out of malfunctioning of sensors can play a vital role .

It is to be observed that some of the above factors may not have any role to affect repeatability because the inaccuracy in such cases may be repeatable .

1.3 LITERATURE REVIEW

The vibration in a moving flexible Robot arm was considered by Wang et al [1]. They have shown how the extension and contraction motions have destabilizing and stabilizing effects on the vibratory motion respectively . The vibration analysis was

based on Galerkin approximation with time dependent basis function. The study restricted its consideration to the bending vibration of the Robot arm in one plane only.

Meghdhari and Shahinpoor [3] presented a complete derivation of the combined flexural-joint stiffness matrix and the elastic deformation field of a flexible manipulator. The stiffness properties were derived directly from the differential equations used in engineering beam theory. The elasticity of the joint was modelled by considering the robotic links attached end-to-end with the help of flexible connector.

Hill and Vaccaro [4] treated a robotic manipulator with joint compliance to make an on-line scheme for computing the inverse joint solution with non-linear feedback control in joint space . The study used the recursive formulation scheme for calculation of all the elements in the dynamic equation and considered the vibration effect on the feedback loop. It neglected the existence of Coulomb friction and gear backlash in the joints. Hence, some error is introduced due to the absence of non-linear contribution from these terms.

Sira-Ramirez et al [5] studied the robust control of robotic manipulator with flexible joints. They modelled the flexibility in the joint by incorporating the concept of "fictitious link" which would take care of the compliance by

converting an 'n' D.O.F manipulator to a corresponding '2n' D.O.F manipulator.

The compliance of a structure varies with the weight it possesses. The lesser weight of a manipulator makes it more vibration-prone as the joint compliance starts taking vital role. In this respect, the vibratory characteristics of an unloaded industrial Robot with rigid links and resilient joints have been highlighted by Sunada et al [5].

Ziegler [6], Bungay et al [7] reported that certain classes of mechanical systems when subjected to non-conservative forces might execute different types of motions like small oscillation, flutter and divergence when disturbed from an equilibrium state. They dealt with mathematical models based on rigid links and resilient joints in an initially straight line configuration.

The above work was followed and improved by Anderson [8]. He investigated the stability of a manipulator subjected to a non-conservative force applied at the free extremity. It includes the different modes of failure of the structure by instability and the computation of the numerical values of the critical divergence and flutter loads for various configurations of the manipulator. They did not consider frictional damping in the joints. By considering a 3_D.O.F planar

manipulator, it lost the generality of spatial motion of a practical-purpose robot.

1.4 PRESENT WORK

The present work attempts to model the robot with the base affected by -

a> Deterministic excitation

b> Random(Stochastic) excitation

The positional inaccuracies induced due to the vibration transmitted to the end effector have been examined for a simple two D.O.F as well as five and six D.O.F robots separately. A small amount of damping that can play the role of controlling response at all values of frequency ratio is included in the analysis. To make it more general, the work has been extended considering PUMA_560 which has six non-redundant links. It also includes the study of the behavior of the manipulator under a constant load at the tip and assorted excitations at the base by giving sinusoidal, square and random input. By all these, a prediction can reasonably be made about the response characteristics of the manipulator when subjected to other general types of dynamic loads. The critical divergence load i.e the load under which one or more natural frequencies cease, bringing about instability in the system is examined at different geometric configurations of the structure. Also its variation with the load at the tip and with

different configurations are plotted to draw a general conclusion about the features of the system at some specific values of joint parameters of the structure. Finally, a comparison of response has been made amongst different D.O.F manipulators for random input excitation .

CHAPTER 2

MODELLING

2.1 ASSUMPTIONS

We have modelled a simple 2_D.O.F manipulator as well as five and six D.O.F manipulators separately with flexible joints. The links are connected end to end through revolute joints. The link connecting actuator to the arm undergoes re tive rotation with respect to its two ends. This flexibility at the joint is modelled by linear torsional spring with spring constant 'K'.

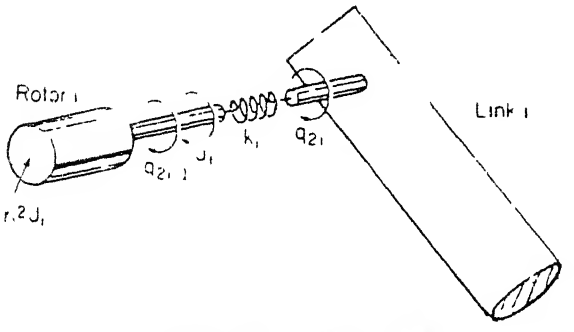

FIG.2.1 ELASTIC JOINT.

The model is based on these assumptions .

1> The links are totally rigid except the compliance at the joints.

2> The links are cylindrical and axisymmetric .

3> The mass density of the links are uniform .

4> The joints may undergo small oscillations .

5> The motion of the manipulator about the equilibrium configuration is very slow. The same assumption was followed by Anderson[8].

2.2 LINK CO-ORDINATE SYSTEM ASSIGNMENT

For the study of response, it is always convenient to set up individual co-ordinate frames to each link. Each frame will be related to the non-inertial base frame by link and joint parameters. To set up the co-ordinate frames, Denavit-Hartenberg convention [1,3] is followed as given below.

With reference to Fig.3 , it can be written

1. The Z_{n-1} axis lies along the axis of motion of the n^{th} joint.
2. The x_n axis is normal to the z_{n-1} axis and pointing away from it in the direction of the common normal of z_{n-1} and z_n axes.
3. The y_n axis completes the right handed co-ordinate system as required.

By this, one is free to choose the location of $zero^{th}$ co-ordinate frame anywhere in the supporting base, as long as the x_n axis is normal to the z_n axis .

2.3 TRANSFORMATION MATRIX

Let the transformation matrix between the i^{th} and the $(i-1)^{th}$ frames be given by $\left[{}^{i-1}T_i\right]$. Also $\sin(\theta n)$, $\cos(\theta n)$ are denoted by Sn, Cn and $\sin(\phi m)$, $\cos(\phi m)$ by Sm, Cm respectively where m = 2,3,6 and n = 1,4,5.

Thus,

$$\left[{}^{B}T_{O}\right] = \text{Trans}\left[0,0,Z_B\right] = \begin{bmatrix} 1 & 0 & 0 & 0 \\ 0 & 1 & 0 & 0 \\ 0 & 0 & 1 & Z_B \\ 0 & 0 & 0 & 1 \end{bmatrix}$$

$$\left[{}^{O}T_{1}\right] = \left[\text{ROT}\left(Z,\theta_1\right)\right]*\left[\text{Trans}\left(0,0,L_1\right)\right]*\left[\text{ROT}\left(Y,90^{\circ}\right)\right]*\left[\text{ROT}\left(Z,180^{\circ}\right)\right]$$

$$= \begin{bmatrix} 0 & S_1 & C_1 & 0 \\ 0 & -C_1 & S_1 & 0 \\ 1 & 0 & 0 & L_1 \\ 0 & 0 & 0 & 1 \end{bmatrix}$$

$$\left[{}^{B}T_{1}\right] = \left[{}^{B}T_{O}\right]*\left[{}^{O}T_{1}\right] = \begin{bmatrix} 0 & S_1 & C_1 & 0 \\ 0 & -C_1 & S_1 & 0 \\ 1 & 0 & 0 & (L_1 + Z_B) \\ 0 & 0 & 0 & 1 \end{bmatrix}$$

Where, $\left[\text{ROT}\left(\text{axis}_1,\theta_1\right)\right]$ denotes the rotation about any axis 'axis1' by an angle θ_1 and $\left[\text{Trans}\left(x,y,z\right)\right]$ denotes a translation of x along X axis, y along Y axis and z along Z axis

$$\left[{}^{1}T_{2}\right] = \left[\text{ROT}\left(Z,\theta_2\right)\right]*\left[\text{Trans}\left(L_2,0,0\right)\right] = \begin{bmatrix} C_2 & -S_2 & 0 & L_2*C_2 \\ S_2 & C_2 & 0 & L_2*S_2 \\ 0 & 0 & 1 & 0 \\ 0 & 0 & 0 & 1 \end{bmatrix}$$

$$\left[{}^{B}T_{2}\right] = \left[{}^{B}T_{1}\right]*\left[{}^{1}T_{2}\right]$$

Now putting $\theta_2 = (\Phi_2 - \Pi/2)$ where Φ_2 is the angle made by the 2^{nd}

link with the horizontal, we get

$$\left[{}^{B}T_{2}\right] = \begin{bmatrix} -S_1*C_2 & S_2*C_1 & C_1 & -L_2*S1*C_2 \\ -C_1*C_2 & -S_2*C_1 & S_1 & L_2*C1*C_2 \\ S_2 & C_2 & 0 & (L_1 + L_2*S_2 + Z_B) \\ 0 & 0 & 0 & 1 \end{bmatrix}$$

$$\left[{}^{2}T_{3}\right] = \left[\text{ROT}(Z, \Phi_3-\Phi_2)\right]*\left[\text{ROT}(X, -90^\circ)\right]*\left[\text{ROT}(Y, 90^\circ)\right]$$

$$\left[{}^{B}T_{3}\right] = \left[{}^{B}T_{2}\right]*\left[{}^{2}T_{3}\right]$$

$$= \begin{bmatrix} -S_1*S_3 & -C_1 & -S_1*C_3 & (-L_2*S1*C_2) \\ C_1*S_3 & -S_1 & C_1*C_3 & (L_2*C_1*C_2) \\ -C_3 & 0 & S_3 & (L_1 + L_2*S_2 + Z_B) \\ 0 & 0 & 0 & 1 \end{bmatrix}$$

$$\left[{}^{3}T_{4}\right] = \left[\text{ROT}(Z, \theta_4)\right]*\left[\text{Trans}(0, 0, L_3+L_4)\right]*\left[\text{ROT}(X, 90^\circ)\right]$$

$$\left[{}^{B}T_{4}\right] = \left[{}^{B}T_{3}\right]*\left[{}^{3}T_{4}\right]$$

$$
= \begin{bmatrix}
[S_1 S_3 C_4 + C_1 S_4] & -[S_1 C_3] & [-S_1 S_3 S_4 + C_1 C_4] & \\
[S_3 C_1 C_4 - S_1 S_4] & [C_1 C_3] & [S_3 S_4 C_1 + S_1 C_4] & \\
[-C_3 C_4] & [S_3] & [-S_4 C_3] & \\
[0] & [0] & [0] & \\
 & & -S_1[(L_3+L_4)C_3 + L_2 C_2] & \\
 & & C_1[(L_3+L_4)C_3 + L_2 C_2] & \\
 & & [(L_3+L_4)S_3 + L_1 + L_2 S_2 + Z_3] & \\
 & & [1] &
\end{bmatrix}
$$

$$
\left[{}^{4}T_{5}\right] = \left[\mathrm{ROT}(Z, \theta_5)\right] * \left[\mathrm{ROT}(X, -90^\circ)\right]
$$

$$
= \begin{bmatrix}
C_5 & 0 & -S_5 & 0 \\
S_5 & 0 & C_5 & 0 \\
0 & -1 & 0 & 0 \\
0 & 0 & 0 & 1
\end{bmatrix}
$$

$$\left[{}^{0}T_{5}\right] = \left[{}^{0}T_{4}\right]*\left[{}^{4}T_{5}\right] =$$

$$\begin{bmatrix}
-[(S_1*S_0*C_4+C_1*S_4)*C_5 + S_1*S_5*C_0] & [S_1*S_0*S_4 - C_1*C_4\ ] \\
[(S_0*C_1*C_4-S_1*S_4)*C_5 + S_5*C_1*C_0] & -[S_4*S_0*C_1 - S_1*C_4\ ] \\
[-C_5*C_0*C_4+S_0*S_5] & [S_4*C_0] \\
[0] & [0] \\
[(S_1*S_0*C_4+C_1*S_4)*S_5-S_1*C_5*C_0] & [-S_1*\{(L_0+L_4)*C_0+L2*C_2\}] \\
[-(S_0*C_1*C_4-S_1*S_4)*S_5+C_5*C_1*C_0] & [C_1*\{(L_0+L_4)*C_0+L_2*C_2\}] \\
[S_5*C_0*C_4 + S_0*C_5\ ] & [(L_0+L_4)*S_0+L_1+L_2*S_2+Z_0] \\
[0] & [\,1] \\
\end{bmatrix}$$

This chapter has dealt with transformation matrices relating different link co-ordinate frames with that of the base. Thus the potential energy and kinetic energy of the system which is nothing but the summation of the same of the individual links, can be found out with great ease in the next chapters 3 and 4.

CHAPTER 3

DYNAMICAL EQUATIONS OF A TWO DEGREE OF FREEDOM MANIPULATOR

Before going to the complexity of a 6_D.O.F robot, let us take the case of a 2_D.O.F robot and analyze it to get an insight into the problem. In order to find the equations of motion, the potential and the kinetic energy of the system at any arbitrary configuration is desired.

3.1: KINETIC ENERGY (KE) CALCULATION

A> KE OF THE FIRST LINK

With reference to Fig.2.1, it can be shown that

$$\left[{}^{B}\rho_1\right] = \left[{}^{B}T_1\right]*\left[{}^{1}\rho_1\right] = \begin{bmatrix} Y*S_1 + Z*C_1 \\ -Y*C_1 + Z*S_1 \\ -X + L_1 + Z_B \\ 1 \end{bmatrix}$$

where,

$\left[{}^{1}\rho_1\right] = \left[\,-X \quad Y \quad Z \quad 1\,\right]^{T}$, denoting the position vector of any point on link1 with respect to the 1^{st} co-ordinate frame.

By differentiating, we get

$$\left[{}^{B}\dot{\rho}_1\right] = \begin{bmatrix} (Y*C_1 - Z*S_1)*\dot{\theta}_1 \\ (Y*S_1 + Z*C_1)*\dot{\theta}_1 \\ \dot{Z}_B \\ 0 \end{bmatrix}$$

Let KE_1 denote the kinetic energy of link 1.

$$KE_1 = 0.5*\sum_{m1}\left({}^{B}Vel_1\right)^2 * dm$$

Where,

$\left[{}^{B}Vel_1\right]$ is the velocity of the first link with respect to the base frame.

Now,

$$\left[{}^{B}Vel_1\right]^2 = \begin{bmatrix} B\dot{\rho}_1 \end{bmatrix}^T \begin{bmatrix} B\dot{\rho}_1 \end{bmatrix} = (\dot{\theta}_1)^2 * \begin{bmatrix} Y^2 + Z^2 \end{bmatrix} + (\dot{Z}_B)^2$$

Therefore,

$$KE_1 = 0.5 * \sum_{m1} \left[(Y^2 + Z^2) * (\dot{\theta}_1)^2 + (\dot{Z}_B)^2 \right] * dm$$

$$= 0.5 * J_1 * (\dot{\theta}_1)^2 + 0.5 * m_1 * (\dot{Z}_B)^2$$

Where,

J_1 is the polar moment of inertia of the 1st link.

B) KINETIC ENERGY OF THE SECOND LINK:

The position vector of any point on link2 in the base frame is

$$\left[{}^{B}\rho_2\right] = \left[{}^{B}T_2\right] * \left[{}^{2}\rho_2\right] = \begin{bmatrix} X*S_1*C_2 + Y*S_1*S_2 + Z*C_1 - L_1*S_1*C_2 \\ Z*S_1 - X*C_1*C_2 - Y*S_2*C_1 + L_2*C_2*C_1 \\ Y*C_2 - X*S_2 + L_1 + L_2*S_2 + Z_B \\ 1 \end{bmatrix}$$

where,

$$\left[{}^{2}\rho_2\right] = \begin{bmatrix} -X \\ Y \\ Z \\ 1 \end{bmatrix}$$

Now ,

$$KE_2 = 0.5 * \sum_{m_2} \left[{}^{B}Vel_2 \right]^2 * dm$$

Where,

$\left[{}^{B}Vel_2 \right]$ is the velocity of the second link with respect to the base frame.

$$\left[{}^{B}Vel_2 \right] = (\dot{\theta}_1)^2 * \left[I_{xx}^2 * (s_2)^2 + I_{yy}^2 * (C_2)^2 \right] + I_{zz}^2 * (\dot{\Phi}_2)^2 + (\dot{Z}_B)^2 * m_2$$

$$- (\dot{\theta}_1) * (\dot{\Phi}_2) * C_2 * M_2 * L_2^2 * 0.5 + (\dot{\Phi}_2) * (\dot{Z}_B) * C_2 * m_2 * L_2$$

Here, I_{xx}^2 is the moment of inertia of the second link with respect to the X_2 axis and I_{yy}^2 is the same with respect to the Y_2 axis.

3.2 :POTENTIAL ENERGY(PE) CALCULATION

The potential energy of any link would consist of two parts. One would be coming from the conservative forces due to gravity and the other would be from spring force due to joint compliance . As the n^{th} joint is rotated through an angle ϕ_n, a restoring moment of $k_n * \Phi_n$ is induced in the joint. This is contributing to increase in P.E.of the system. The potential energy of the system(PE_{sys}) can be written as the summation of the potential energies of the first and the second links.

$$PE_{sys} = PE_1 + PE_2$$

$$= M_1 * g * (0.5 * L_1 + Z_B) + M_2 * (L_1 + Z_B + 0.5 * L_2 * S_2) * g$$

$$+ 0.5 * K_2 * (\phi_2 - \phi_{20})^2 + 0.5 * K_1 * (\theta_1 - \theta_{10})^2$$

Where ϕ_{2o} and θ_{1o} are the equilibrium angles of link2 and link1 respectively. K2 and K1 denote the rotational stiffness of the respective joints.

3.3 LAGRANGE'S EQUATION

Lagrange s equation in terms of generalised force and co-ordinate is

$$\frac{d}{dt}\left(\frac{\partial L}{\partial \dot{q}_k}\right) - \frac{\partial L}{\partial q_k} = Q_k$$

or,
$$\frac{d}{dt}\left(\frac{\partial T}{\partial \dot{q}_k}\right) - \frac{\partial T}{\partial q_k} + \frac{\partial V}{\partial q_k} = Q_k. \quad \ldots\ldots\ldots\ldots\ldots\ldots\ldots\ldots (3.1)$$

Where,

L is called the Lagrangean and L= (KEsys - PEsys)

q_k and Q_k are the generalised co-ordinate and force respectively.

3.4 CALCULATION OF GENERALISED FORCES

Let us choose Z_B , θ_1, and ϕ_2 to be the generalised co-ordinates.The corresponding generalised forces are Q_B, Q_1 and Q_2. When there is a virtual displacement in the system from the equilibrium configuration, the virtual work done(vwd) is given by

$$VWD = (U_1 - T_{f1})*d\theta_1 + (U_2 - T_{f2})*d\phi_2 + \vec{P}.d\vec{R}_p$$

Where $\vec{R}_p$ is the position vector of the end efector tip with respect to the base frame and U_1, U_2 are the joint torques of the respective joints. T_{f1} and T_{f2} are the frictional torques at the joints .

$$\vec{R}_p = -L_2*C_2*S_1*\hat{j} + L_2*C_2*C_1*\hat{j} + (L_1 + L_2*S_2 + Z_B)*\hat{k}$$

Where $\hat{i}, \hat{j}, \hat{k}$ are the unit vectors along X_B, Y_B, Z_B axis.

Now , $\vec{P} = -P*\hat{K}$

Hence,

$$\vec{P}.d\vec{R}_P = -P*L_2*C_2*d\phi_2 - P*dZ_B$$

$$VWD = (U_1 - T_{f1})*d\theta_1 + (U_2 - T_{f2} - P*L_2*C\phi_2)*d\phi_2 - P*Z_B$$

So, the generalised forces are :

$$Q_1 = U_1 - T_{f1}$$

$$Q_2 = U_2 - T_{f2} - P*L_2*C_2$$

$$Q_B = -P$$

3.5 EQUATION OF MOTION

In order to find the equation of motion,Lagrange s equation is used for each of the generalised co-ordinates .Taking Q_1 and θ_1 as the generalised force and co-ordinate respectively, after going through some mathematical operations, we get.

$$U_1 = 0 \quad \ldots\ldots\ldots\ldots\ldots\ldots\ldots\ldots\ldots\ldots\ldots\ldots 3.2$$

Similarly, taking Q_2 and ϕ_2, the corresponding equation is

$$\ddot{\phi}_2*^2 I_{ZZ} + \frac{1}{2}*\ddot{Z}_B*M_2*L_2*C_2 + K_2*(\phi_2 - \phi_{2O}) + \frac{1}{2}*M_2*L_2*g*C_2$$
$$= U_2 - P*L_2*C_2 - T_{f2} \quad \ldots\ldots\ldots\ldots\ldots\ldots 3.3$$

Taking Q_B and Z_B,

$$(M_1 + M_2)\ddot{Z}_B + 0.5*M_2*L_2*C_2*\ddot{\phi}_2 - 0.5*M_2*L_2*S_2*(\dot{\phi}_2)^2$$
$$+ (M_1 + M_2)*g = -P \quad \ldots\ldots\ldots\ldots\ldots\ldots 3.4$$

The first of these equations shows that the external torque to be applied in the first joint is zero because there is no disturbing couple in the axial direction of

the first link .

The second equation is actually the vibration equation taking care of the spring ,damping and external forces.

The third one is coming from the dynamic equilibrium of the structure by considering the force balance in the vertical direction.

3.6 SIMPLIFICATION

In this section, some simplifying assumptions have been made that will permit the reduction of the complexity of the differential equation 3.3 . It is assumed that the system is in a state of equilibrium when $\phi_2 = \phi_{20}$ and $\theta_1 = \theta_{10}$ with Uk's denoting the torques applied at the joints.

At equilibrium configuration, equation (3.3) reduces to

$$M_2 * L_2 * g * C_{20} * 0.5 = U_2 - P * L_2 * C_{20}$$

Now, as mentioned earlier, the motion of the manipulator being small about the equilibrium configuration, one can write

$$\phi_k(t) = \phi_{ko} + \phi_{kk}(t), \text{ where } |\phi_{kk}| << 1$$

In particular, it is assumed that one can make the approximation

$$\cos(\phi_{kk}) \tilde{=} 1$$

$$\sin(\phi_{kk}) \tilde{=} \phi_{kk}$$

Therefore,

$$\sin(\phi_k) \tilde{=} \sin(\phi_{ko}) + \phi_{kk} * \cos(\phi_{ko})$$

analogously,

$$\cos(\phi_k) \tilde{=} \cos(\phi_{ko}) - \phi_{kk} * \sin(\phi_{ko})$$

The terms like $\phi k * \ddot{Z}_B$ are ignored.

By using these simplifying assumptions, it can be written,

$$I_{zz}^2 * \ddot{\phi}_{z2} + C_{zd} * \dot{\phi}_{z2} + \left[K_z - (M_z * g * 0.5 + P) * L_z * S_{zo} \right] * \phi_{z2} = - \frac{M_z * L_z * C_{zo} * \ddot{Z}_B}{2}$$

$$\ddot{\Phi}_z + 2 * \xi * \omega_n * \dot{\phi}_{z2} + \omega_n^2 * \phi_{z2} = \frac{M_z * L_z * C_{zo} * \ddot{Z}_B}{2 * I_{zz}^2} \quad \ldots\ldots\ldots\ldots\ldots 3.5$$

Where,

$$\omega_n^2 = \frac{K_z - (M_z * g * 0.5 + P) * L_z * S_z}{I_{zz}^2}$$

$$\xi = \frac{C_{zd}}{2 * I_{zz}^2 * \omega_n}$$, C_{zd} being the damping co-efficient .

3.7 DETERMINISTIC EXCITATION

3.7.1 : SINUSOIDAL EXCITATION

Let sinusoidal excitation acts at the base of the manipulator and is given by $Z_B = Z_o * \sin(\omega * t)$, where Z_o is the amplitude and ω is the frequency of the forced excitation .

Hence, equation **3.5.** can be written as

$$\ddot{\phi}_{z2} + 2 * \xi * \omega_n * \dot{\phi}_{z2} + \omega_n^2 * \phi_{z2} = V * \sin(\omega * t) \quad \ldots\ldots\ldots\ldots\ldots 3.6$$

Where $V = M_z * L_z * C_z * Z_o * \omega^2 / (2 * I_{zz}^2)$

The above equation **3.6** has to be solved for the transient as well

as steady state.

The three transient solutions depend upon the value of ξ.

CASE 1: $\xi > 1$

$$\phi 22_{/trans} = e^{-(decay*t)} * [C1*e^{(dfq*t)} + C2*e^{-(dfq*t)}]$$

CASE 2: $\xi < 1$

$$\phi 22_{/trans} = e^{-(decay*t)} * [C1*\cos(dfq*t) + C2*\sin(dfq*t)]$$

CASE 3: $\xi = 1$

$$\phi 22_{/trans} = (C1 + C2*t)*e^{-(\omega n*t)}$$

The particular integral is

$$PI = A*\sin(\omega*t + \phi)$$

Where, $A = V/\left[\sqrt{\left[1 - (\omega/\omega n)^2\right]^2 + (2*\xi*\omega/\omega n)^2}\right]$

$$\phi = \tan^{-1}\left[2*\xi*\omega/\omega n/\left[(\omega/\omega n)^2 - 1\right]\right]$$

Hence the complete solution is

$$\phi 22 = \phi 22_{/trans} + PI .$$

As the response of the second joint is known , the response of the end effector can be found out with respect to the base co-ordinate frame . The vibrations in the X_B, Y_B, Z_B directions are given by

$$Ei = - L2*S10*S20*\phi 22$$

$$Ej = L2*C10*S20*\phi 22$$

$Ek = L_2 * C_{20} * \phi_{22} + Z_B$

3.7.2 SQUARE IMPULSE EXCITATION

A square impulse excitation at the base having an Amplitude of Zo and period 'tt' is assumed to act at the base of the robot. The pulse can be represented with the help of Fourier series as follows:-

$$Z_B = Z_{av} + \frac{2*Z_o}{\Pi} \sum_{n=1}^{\infty} \frac{1}{n} * \sin\left[\frac{\Pi * n * t_1}{tt}\right] * \cos\left[\frac{\Pi * t_1 * n}{tt} - \frac{2\Pi * n * t}{tt}\right] \text{--------} 3.7$$

Hence, the solution of equation 3.5 with square input of the above type is given by:

$$\phi_{22} = \phi_{22/trans} + \sum_{n=} \frac{AMP_n}{\omega_n^2} * \sin\left[\frac{2\Pi * n * t}{tt} + LAG_n\right]$$

Where ,

$\phi_{22/trans}$ is same as before .

$$\text{and} \quad LAG_n = \frac{\Pi}{2} - \frac{\Pi * n * t_1}{tt} + \tan^{-1}\left[2 * \xi * (\omega_{fn}/\omega_n) / \left((\omega_{fn}/\omega_n)^2 - 1\right)\right]$$

Where, $\omega_{fn} = 2\Pi * n/tt$

The response of the end effector can be found using the same expressions as in the case of sinusoidal excitations .

3.8 : RANDOM EXCITATION

3.8.1 : ASSUMPTIONS

Let us now consider random excitation at the base of the manipulator . Any random process can be characterized by the

probability density and distribution functions such that spectral density , auto-correlation function , mean square value etc.. The most general type of random excitation is too complex but some of the random processes have been studied extensively in literature [13—15] with respect to vibration problems. The random process under consideration is based on some assumptions. These are

1· The random process is ergodic and stationary .

2) It follows baussian distribution .

3) The spectral density of excitation is constant over feasible range of frequency .

3.8.2 COMPLEX RECEPTANCE

Let the spectral density of excitation be denoted by S_p .In order to find the spectral density of response at the tip,the complexreceptance of the system is to be found out. Let it be denotedby $\alpha(i\omega)$. Hence, for a load of $Z_B = Z_o * e^{i\omega t}$,with the help of equation.3.5 the response of the second joint can be written as $\phi_{22} = \alpha(i\omega) * Z_o * e^{i\omega t}$.

Where,

$$\alpha(i\omega) = {}^{2}I_{zz} * \left[\frac{0.5 * M_2 * L_2 * C_{2o} * \omega^2}{(\omega_n^2 - \omega^2) + i * 2 * \xi * \omega * \omega_n} \right] \quad \text{---------} \quad 3.8$$

$$= \alpha_r - i * \alpha_m$$

Where,

$$\alpha_r = \frac{M_2 * L_2 * C_{20} * \omega^2 * (1 - F_r^2)}{2 * \zeta^2 I_{zz} * \left[(1 - F_r^2) + (2 * \zeta * F_r)^2 \right]}$$

F_r , the frequency ratio $= \frac{\omega}{\omega_n}$

and,

$$\alpha_{im} = \frac{M_2 * L_2 * C_{20} * \omega^2 * 2 * \zeta * F_r}{2 * \zeta^2 I_{zz} * \left[(1 - F_r^2) + (2 * \zeta * F_r)^2 \right]}$$

3.8.3 : SPECTRAL DENSITY OF THE RESPONSE

After the complex receptance of the system is known, the spectral density of the response can be related to that of excitation .

The response of the end effector in the vertical direction for any Z_B is given by ,

$$E_k = L_2 * C_2 * \phi_{22} + Z_B$$

$$= \left[L_2 * C_2 * \alpha(i\omega) + 1 \right] * Z_o * e^{i\omega t}$$

$$E_k = E_k(i\omega) * Z_o * e^{i\omega t}$$

$$= (E_{kr} - i * E_{kim}) * Z_o * e^{i\omega t}$$

Where,

$$E_{kr} = 1 + L_2 * C_{20} * \alpha_r$$

and

$$E_{kim} = L_2 * C_{20} * \alpha_{im}$$

Hence,

$$|E_k(i\omega)|^2 = E_{kr}^2 + E_{kim}^2$$

Similarly, for the Y component of response

$$|E_j(i\omega)|^2 = (E_{jr})^2 + (E_{jim})^2$$

$$E_{jr} = - L_2 * S_2 * C_1 * \alpha_r$$

$$E_{jim} = - L_2 * S_2 * C_1 * \alpha_{im}$$

And finally for the X-component,

$$|E_i(i\omega)|^2 = (E_{ir})^2 + (E_{iim})^2$$

$$E_{ir} = L_2 * S_2 * S_1 * \alpha_r$$

$$E_{iim} = L_2 * S_2 * S_1 * \alpha_{im}$$

The spectral density of response in any direction n' may be expressed as

$$S_n(\omega) = |E_n(i\omega)|^2 * S_p(\omega)$$

3.8.4 MEAN SQUARE VALUE OF THE RESPONSE

The mean square value of the response of the end effector can be found by the following integral-

$$\langle E_n^2(t) \rangle = \frac{1}{2*\Pi} * \int_0^{\infty} |E_n(i\omega)|^2 * S_p * d\omega$$

$$\langle E_n^2(t) \rangle = \frac{S_p}{2*\Pi} * \int_0^{\infty} |E_n(i\omega)|^2 * d\omega$$

The above integral of the mean square value can be calculated with the help of Residue Theory or by any standard procedure of numerical integration [10].

For a linear system ,if the input excitation follows Gaussian distribution ,the response will also follow the same distribution [13] .

As the system under consideration is linear , by making use of

this property, after assuming zero mean of the response one can write, $P(En) = \frac{1}{\sigma * \sqrt{(2*\Pi)}} * e^{-En^2/2\sigma n^2}$

Where, $\sigma n^2 = \langle En(t)^2 \rangle$ and is called the variance.

3.9 SUMMARY

This chapter has described the position of the end effector of a 2_D.O.F robot at any joint configuration. Thus the deviation of the end effector from a particular desired position can be obtained at any instant of time. The behavior of the response of the end effector at various frequencies and spectral density is shown in chapter 5.

CHAPTER 4

DYNAMICAL EQUATIONS OF MULTI-DEGREE-FREEDOM MANIPULATORS

4.1 5_D.O.F SYSTEM

4.1.1 : K.E AND P.E CALCULATION

Following the same procedure as depicted in chapter 3, one can arrive at the expressions of the K.E and P.E of the 3^{rd}, 4^{th} and the 5^{th} links as follows

$$(K.E)_3 = \frac{1}{2}*\left[{}^{3}I_{zz}\right]*(\dot{\phi}_3)^2 + \frac{1}{2}*M_3*L_2^2*(\dot{\phi}_2)^2 + M_3*L_2*C_2*\dot{\phi}_2*\dot{Z}_3$$

$$+ \frac{1}{2}*M_3*L_2*L_3*\cos(\phi_2-\phi_3)*\dot{\phi}_2*\dot{\phi}_3 + \frac{1}{2}*M_3*L_3*C_3*\dot{Z}_3*\dot{\phi}_3$$

$$(P.E)_3 = \frac{1}{2}*K_3*\left[\phi_3 - \phi_{30} + \phi_{20} - \phi_2\right]^2$$

$$+ \left[L_1 + Z_3 + L_2*S_2 + \frac{L_3}{2}*S_3\right]*M_3*g$$

$$(K.E)_4 = \frac{1}{2}*M_4*L_2^2*(\dot{\phi}_2)^2 + \frac{1}{2}*{}^{4}I_{yy}*(\dot{\phi}_4)^2 + \frac{1}{2}*M_4*(\dot{Z}_3)^2$$

$$+ M_4*L_2*C_2*\dot{\Phi}_2*\dot{Z}_3 + M_4*L_2*\left(L_3 + \frac{L_4}{2}\right)*C_{32}*\dot{\Phi}_2*\dot{\Phi}_3$$

$$+ M_4*\left(L_3 + \frac{L_4}{2}\right)*C_3*\dot{\phi}_3*\dot{Z}_3 + I_{eq}*(\dot{\phi}_3)^2$$

Where,

$$I_{eq} = 0.5*{}^{4}I_{xx} + 0.5*M_4*(L_3 + {}_4)^2 - 0.5*M_4*L_4*(L_3 + L_4)$$

$$+ 0.125*M_4*L_4^2*\sin(2\theta_4).$$

$$(P.E)_4 = M_4*g*\left[\dot{Z}_B + L_1 + L_2*S_2 + (L_3 + 0.5*L_4)*C_3\right] + 0.5*K_4*(\theta_4 - \theta_{40})^2$$

$$(K.E)_5 = 0.5*M_5*L_2^2*(\dot{\phi}_2)^2 + 0.5*\left[C_5^2*{}^5I_{zz} + S_5^2*{}^5I_{yy}\right]*(\dot{\phi}_4)^2$$

$$+ 0.5*\left[(S_4*S_5)^2*{}^5I_{zz} + \left((S_4*C_5)^2 + C_4^2\right)*{}^5I_{yy} + M_5*(L_3+L_4)^2\right.$$

$$\left. - \frac{M_5*L_5^2}{4}*\sin(2\theta_4)*C_5 + M_5*L_5*(L_3 + L_4)*C_5\right]*(\dot{\phi}_3)^2 +$$

$$\frac{1}{2}*{}^5I_{yy}*(\dot{\phi}_5)^2 + \left[\frac{M_5*L_2*L_5}{2}*(C_5*C_{32} - S_5*C_4*S_{32}) + M_5*L_2(L_3+L_4)*C_{32}\right]\dot{\phi}_2*\dot{\phi}_3$$

$$- \frac{M_5*L_2*L_5}{2}*\left[S_4*S_5*C_{32}*\dot{\phi}_2*\dot{\phi}_4 - (C_{32}*C_4*C_5 - S_{32}*S_5)\dot{\phi}_2*\dot{\phi}_5\right] +$$

$$\left[S_4*S_5*C_5*{}^5I_{yy} + S_5*C_4*\frac{M_5*L_5^2}{4} - \frac{M_5*L_5*(L_3 + L_4)}{2}*S_4*S_5\right]*\dot{\phi}_3*\dot{\phi}_4 +$$

$$\left[C_4*{}^5I_{yy} - S_4*C_5*\frac{M_5*L_5^2}{4} + \frac{M_5*L_5*(L_3+L_4)}{2}*C_4*C_5\right]*\dot{\phi}_3*\dot{\phi}_5 + S_5*\frac{L_5^2*M_5}{4}*\dot{\phi}_4*\dot{\phi}_5$$

$$+\left[(C_3*C_5 - S_3*S_5*C_4)*\frac{M_5*L_5}{2} + M_5*(L_3 + L_4)*C_3\right]*\dot{\phi}_3*\dot{Z}_B + M_5*L_2*C_2*\dot{\phi}_2*\dot{Z}_B$$

$$+ \frac{M_5*L_5}{2}*\left[(C_3*C_4*C_5 - S_3*S_5)*\dot{\phi}_5*\dot{Z}_B - S_4*S_5*C_3*\dot{\phi}_4*\dot{Z}_B\right] + 0.5*M_5*(\dot{Z}_B)^2$$

$$(P.E)_5 = M_5*g*\left[Z_B + L_1 + L_2*S_2 + (L_3 + L_4)*S_3 + \frac{L_5}{2}*(S_5*C_3*C_4 + S_3*C_5)\right] + \frac{1}{2}*K_5*(\theta_5 - \theta_{50})^2$$

4.1.2 CALCULATION OF GENERALIZED FORCES

Let the generalized co-ordinates are θ_1, ϕ_2, ϕ_3, θ_4, θ_5, and

Z_B.The corresponding generalized forces are Q_1, Q_2, Q_3, Q_4, Q_5 and Q_B. Using the same procedure as that of the 2_D.O.F robot, one can obtain the generalized forces for a 5-D.O.F system.

Thus,

$Q_1 = U_1$

$Q_2 = U_2 - U_3 - P*L_2*C\phi_2$

$Q_3 = U_3 - P*[(L_3 + L_4)*C_3 - L_5*S_3*S_5*C_4 + L_5*C_3*C_5]$

$Q_4 = U_4 + P*L_5*S_4*S_5*C_3$

$Q_5 = U_5 - P*L_5*[C_3*C_4*C_5 - S_3*S_5]$

$Q_B = - P$

4.1.3 : EQUATION OF MOTION

Applying Lagrange s equation for each of the independent co-ordinates, one can get the equation of motion of the system. Considering the equilibrium of the system at $\phi_k = \phi_{ko}$, applying the standard technique for linearisation and neglecting the terms like $\dot{\phi}_j*\dot{\phi}_k$ and $(\dot{\phi}_j)^2$, the set of coupled linear equations obtained are given below.

$$M_{11}*\ddot{\phi}_{22} + M_{12}*\ddot{\phi}_{33} + M_{13}*\ddot{\phi}_{44} + M_{14}*\ddot{\phi}_{55} + K_{11}*\phi_{22} + K_{12}*\phi_{33} + K_{13}*\phi_{44} + K_{14}*\phi_{55} = P_1 \quad \ldots\ldots 4.1$$

$$M_{21}*\ddot{\phi}_{22} + M_{22}*\ddot{\phi}_{33} + M_{23}*\ddot{\phi}_{44} + M_{24}*\ddot{\phi}_{55} + K_{21}*\phi_{22} + K_{22}*\phi_{33} + K_{23}*\phi_{44} + K_{24}*\phi_{55} = P_2 \quad \ldots\ldots 4.2$$

$$M_{31}*\ddot{\phi}_{22} + M_{32}*\ddot{\phi}_{33} + M_{33}*\ddot{\phi}_{44} + M_{34}*\ddot{\phi}_{55} + K_{31}*\phi_{22} + K_{32}*\phi_{33} + K_{33}*\phi_{44} + K_{34}*\phi_{55} = P_3 \quad \ldots\ldots 4.3$$

$$M_{41}*\ddot{\phi}_{22} + M_{42}*\ddot{\phi}_{33} + M_{43}*\ddot{\phi}_{44} + M_{44}*\ddot{\phi}_{55} + K_{41}*\phi_{22} + K_{42}*\phi_{33} + K_{43}*\phi_{44}$$

$$+K_{44}*\phi_{55} = P_4 \quad \text{..... 4.4}$$

We can write all these equations in matrix form as follows.

$$[M][\ddot{X}] + [K][X] = [P] \quad \text{..... 4.5}$$

where,

$$[M] = \begin{bmatrix} M_{11} & M_{12} & M_{13} & M_{14} \\ M_{21} & M_{22} & M_{23} & M_{24} \\ M_{31} & M_{32} & M_{33} & M_{34} \\ M_{41} & M_{42} & M_{43} & M_{44} \end{bmatrix}$$

$$[K] = \begin{bmatrix} K_{11} & K_{12} & 0 & 0 \\ K_{21} & K_{22} & K_{23} & K_{24} \\ 0 & K_{32} & K_{33} & K_{34} \\ 0 & K_{42} & K_{43} & K_{44} \end{bmatrix}$$

$$[P] = [P_1 \quad P_2 \quad P_3 \quad P_4]^T$$

$$[X] = [\phi_{22} \quad \phi_{33} \quad \phi_{44} \quad \phi_{55}]^T$$

$$P_1 = -\left(\frac{M_2}{2} + M_3 + M_4 + M_5\right)*L_2*C_{20}*\ddot{Z}_B$$

$$P_2 = -\left[\left\{\frac{M_3*L_3}{2} + M_4*\left(L_3 + \frac{L_4}{2}\right) + M_5\left(L_3 + L_4\right)\right\}*C_{30} + \left(C_{30}*C_{50} - S_{30}*S_{50}*C_{40}\right)*\frac{M_5*L_5}{2}\right]*\ddot{Z}_B$$

$$P_3 = \frac{M_5*L_5}{2}\left(S_{40}*S_{50}*C_{30}\right)*\ddot{Z}_B$$

$$P_4 = -\frac{M_5*L_5}{2}\left(C_{30}*C_{40}*C_{50} - S_{30}*S_{50}\right)\ddot{Z}_B$$

$$M_{11} = \left[{}^{2}I_{zz} + (M_3 + M_4 + M_5)*L_2^2\right]$$

$$M_{12} = M_{21} = M_5*L_2*L_5*(C_{50}*C_{320} - S_{50}*C_{40}*S_{320})*0.5 +$$

$$M_5*L_2*(L_3 + L_4)*C_{320} + \frac{M_3*L_2*L_3}{2}*C_{320} + M_4*L_2*\left(L_3 + \frac{L_4}{2}\right)*C_{320}$$

$$M_{13} = M_{31} = -0.5*M_5*L_2*L_5*S_{40}*S_{50}*C_{320}$$

$$M_{14} = M_{41} = \frac{M_5*L_2*L_5}{2}*(C_{320}*C_{40}*C_{50} - S_{320}*S_{50})$$

$$M_{22} = {}^{3}I_{zz} + (S_{40}*S_{50})^2*{}^{5}I_{zz} + \left[(S_{40}*C_{50})^2 + C_{40}^2\right]*{}^{5}I_{yy} + M_5*(L_3 + L_4)^2$$

$$- M_5*L_5*\left[(L_3 + L_4)*C_{50} - \frac{L_5}{4}*\sin(2\theta_{40})*C_{50}\right] + 2*I_{eq}$$

$$M_{23} = M_{32} = S_{40}*S_{50}*C_{50}*{}^{5}I_{yy} + S_{50}*C_{40}*\frac{M_5*(L_5)^2}{4}$$

$$- \frac{M_5*L_5}{2}*(L_3 + L_4)*S_{40}*S_{50}$$

$$M_{24} = M_{42} = C_{40}*{}^{5}I_{yy} - S_{40}*C_{50}*\frac{M_5*(L_5)^2}{4} + 0.5*M_5*L_5*(L_3+L_4)*C_{40}*C_{50}$$

$$M_{33} = {}^{4}I_{yy} + (C_{50})^2*{}^{5}I_{zz} + (S_{50})^2*{}^{5}I_{yy}$$

$$M_{34} = M_{43} = \frac{M_5*(L_5)^2}{4}*S_{50}$$

$$M_{44} = {}^{5}I_{yy}$$

$$K_{11} = K_2 + K_3 - \left[(0.5*M_2 + M_3 + M_4 + M_5)*g + P\right]*L_2*S_{20}$$

$$K_{12} = K_{21} = -K_3$$

$$K_{13} = K_{31} = 0$$

$$K_{14} = K_{41} = 0$$

$$K_{22} = -\left[\left(M_4*(L_3 + 0.5*L_4) + M_5*(L_3 + L_4)\right)*g + P*(L_3 + L_4)\right]*S_{30}$$

$$- \left[S_{50}*C_{30}*C_{40} + S_{30}*C_{50}\right]*\left[P + \frac{M_5*g}{2}\right]*L_5 + K_3 - \frac{M_3*L_3*g}{2}*S_{30}$$

$$K_{23} = K_{32} = S_{30}*S_{40}*S_{50}*\left(P + \frac{M_5*g}{2}\right)*L_5$$

$$K_{24} = K_{42} = -(S_{30}*C_{40}*C_{50} + S_{50}*C_{30})*\left(P + \frac{M_5*g}{2}\right)*L_5$$

$$K_{33} = K_4 - C_{30}*C_{40}*S_{50}*\left(P + \frac{M_5*g}{2}\right)*L_5$$

$$K_{34} = K_{43} = - C_{30}*S_{40}*C_{50}*\left(P + \frac{M_5*g}{2}\right)*L_5$$

$$K_{44} = -(C_{30}*C_{40}*S_{50} + C_{50}*S_{30})*\left(P + \frac{M_5*g}{2}\right)*L_5 + K_5$$

4.1.4 FREE VIBRATION ANALYSIS

Now let us concentrate on the free vibration analysis of the system to obtain a condition from which the system natural frequencies can be found out which would be of much help to know the behavior of the system when subjected to forced vibration.

Let us assume that $[X] = [md]*f(t)$ 4.6

Where, $[md] = \begin{bmatrix} 1 \\ md_1 \\ md_2 \\ md_3 \end{bmatrix}$

Hence by putting this in matrix equation 4.6, we get

$$[M][md]*\ddot{f}(t) + [k][md]*f(t) = [0]$$

$$\frac{\ddot{f}(t)}{f(t)} = \frac{-[md]^T[K][md]}{[md]^T[M][md]} = -\omega^2 \text{ (say)}$$

$$\left[-\omega^2[M] + [K]\right]*[md] = [0]$$

For non-trivial solution of [md] ,

$$\left|-\omega^2[M] + [K]\right| = [0]$$

$$\left|\begin{bmatrix} [K_{11} - \omega^2*M_{11}] & [K_{12} - \omega^2*M_{12}] & [-\omega^2*M_{13}] & [-\omega^2*M_{14}] \\ [K_{21} - \omega^2*M_{21}] & [K_{22} - \omega^2*M_{22}] & [K_{23} - \omega^2*M_{23}] & [K_{24} - \omega^2*M_{24}] \\ [-\omega^2*M_{31}] & [K_{32} - \omega^2*M_{32}] & [K_{33} - \omega^2*M_{33}] & [K_{34} - \omega^2*M_{34}] \\ [-\omega^2*M_{41}] & [K_{42} - \omega^2*M_{42}] & [K_{43} - \omega^2*M_{43}] & [K_{44} - \omega^2*M_{44}] \end{bmatrix}\right| = 0$$

By expanding the above determinant, we get a 8-degree polynomial of the following type.

$$A_0*(\omega)^8 + A_1*(\omega)^6 + A_2*(\omega)^4 + A_3*(\omega)^2 + A_4 = 0 \quad \ldots\ldots\ldots\ldots 4.7$$

Where A_k , $k = 0,1,2,3,4$ are constants to be obtained by expanding the above determinant.

We call this equation as frequency equation.

The solution of the frequency equation would give four pairs of roots that may be real, imaginary or complex. If the external load 'P' at the tip is less than a critical value then the eight roots can be expressed as $\pm\omega_j$, $j = 1,2,3,4$, where $\omega_j > 0$. In such case, the motion of the manipulator is stable. These natural frequencies are functions of the equilibrium angles ϕ_{ko}, $K = 2,3$

and θ_{ko} ,K=1,5 i.e, the natural frequencies of the manipulator depend upon its current geometric configuration. In the description of the numerical calculations that will be reported in chapter [5], indications will be given on how the values of ω_j vary with the equilibrium angles .

4.1.5 : MODAL ANALYSIS

Now our aim is to find the modal vectors corresponding to each of the natural frequencies in a bid to find the mode shapes and later on to obtain the modal matrix which would help enormously to decouple the coupled set of equations [eqn.4.1–4.4] obtained so far. Now, going back to equation, for any ω, we can write

$$(K_{11} - \omega^2 M_{11}) + md_1*(K_{12} - \omega^2 M_{12}) + md_2*(-\omega^2 M_{13}) + md_3*(-\omega^2 M_{14}) = 0 \quad \ldots\ldots 4.8$$

$$(K_{21} - \omega^2 M_{21}) + md_1*(K_{22} - \omega^2 M_{22}) + md_2*(K_{23} - \omega^2 M_{23}) + md_3*(K_{24} - \omega^2 M_{24}) = 0 \quad \ldots\ldots 4.9$$

$$(-\omega^2 M_{31}) + md_1*(K_{32} - \omega^2 M_{32}) + md_2*(K_{33} - \omega^2 M_{33}) + md_3*(K_{34} - \omega^2 M_{34}) = 0 \quad \ldots\ldots 4.10$$

$$(-\omega^2 M_{41}) + md_1*(K_{42} - \omega^2 M_{42}) + md_2*(K_{43} - \omega^2 M_{43}) + md_3*(K_{44} - \omega^2 M_{44}) = 0 \quad \ldots\ldots 4.11$$

Out of these four equations only three are independent and the rest is dependent on these three. This is not at all surprising because at the time of finding the eigen value solution the corresponding determinant was conditionally assumed to be zero.

So one can now solve any three equations to find the modal vectors corresponding to all natural frequencies .

Thus the modal matrix can be written as,

$$[\text{MODE}] = \begin{bmatrix} 1 & 1 & 1 & 1 \\ md_{21} & md_{22} & md_{23} & md_{24} \\ md_{31} & md_{32} & md_{33} & md_{34} \\ md_{41} & md_{42} & md_{43} & md_{44} \end{bmatrix}$$

4.1.6 INCLUSION OF DAMPING:

Let us now incorporate damping in the system. If the damping matrix be denoted by [c], the original matrix equation - 4.5 can be modified as

$$[M][\ddot{X}] + [c][\dot{X}] + [K][X] = [P] \quad \ldots\ldots\ldots\ldots\ldots\ldots\ldots\ldots 4.12$$

To choose a suitable damping matrix for a particular system with reasonable accuracy, is a highly controversial and questionable issue. Because the only way to get a suitable damping matrix is to perform an experiment with the system under consideration, simulating accurately the operating atmosphere of the system and then to evaluate the elements of the damping matrix by proper analysis of the experimental result. Now the first bottleneck that one has to overcome in doing so is to simulate the actual situation in the laboratory which, in most of the cases, is very difficult, if not impossible. The second difficulty lies in measuring all the required experimental result with the level of

accuracy desired. Moreover, even if the experimental results are available, the effort required in performing so hardly satisfies the reliability aspect of it. So some of the very popular empirical approaches are used in practice which at least, seems to be reasonable to strike a balance between the reliability and the effort required in forming them. Author, in the present work has adopted one such approach which considers the damping matrix as a linear combination of mass and stiffness matrix. This approach is suggested by many of the famous persons in the arena of dynamics eg. Clough and Pengien [17].

So, we can write,

$$[c] = c_0*[M] + c_1[K]$$

Putting this in equation [4.12], we get

$$[M][\ddot{X}] + c_0*[M][\dot{X}] + c_1*[K][\dot{X}] + [K][X] = [P] \quad \ldots\ldots 4.13$$

4.1.7 :DECOUPLING

Let $[X] = [MODE][U]$ 4.14

where $[U] = [U_1 \;\; U_2 \;\; U_3 \;\; U_4]^T$

and

U_i's, i=1,2,3,4 are the independent coordinates.

Putting equation 4.14 in equation 4.13 and premultiplying the resulting equation by $[MODE]^T$, we get,

$$[MODE]^T[M][MODE][\ddot{U}] + c_0*[MODE]^T[M][MODE][\dot{U}] + c_1*[MODE]^T[K][MODE][\dot{U}] + [MODE]^T[K][MODE][U] = [MODE]^T[P] \quad \ldots\ldots 4.15$$

Now,

$$[MODE]^{T}[M][MODE] = \begin{bmatrix} NM_{11} & 0 & 0 & 0 \\ 0 & NM_{22} & 0 & 0 \\ 0 & 0 & NM_{33} & 0 \\ 0 & 0 & 0 & NM_{44} \end{bmatrix}$$

Where,

$$NM_{11}=(M_{11} + md_{21}*M_{21} + md_{31}*M_{31} + md_{41}*M_{41}) + (M_{12} + md_{21}*M_{22} + md_{31}*M_{32} + md_{41}*M_{42})*md_{21} + (M_{13} + md_{21}*M_{23} + md_{31}*M_{33} + md_{41}*M_{43})*md_{31} + (M_{14} + md_{21}*M_{24} + md_{31}*M_{34} + md_{41}*M_{44})*md_{41}$$

$$NM_{22}=(M_{11} + md_{22}*M_{21} + md_{32}*M_{31} + md_{42}*M_{41}) + (M_{12} + md_{22}*M_{22} + md_{32}*M_{32} + md_{42}*M_{42})*md_{22} + (M_{13} + md_{22}*M_{23} + md_{32}*M_{33} + md_{42}*M_{43})*md_{32} + (M_{14} + md_{22}*M_{24} + md_{32}*M_{34} + md_{42}*M_{44})*md_{42}$$

$$NM_{33}=(M_{11} + md_{23}*M_{21} + md_{33}*M_{31} + md_{43}*M_{41}) + (M_{12} + md_{23}*M_{22} + md_{33}*M_{32} + md_{43}*M_{42})*md_{23} + (M_{13} + md_{23}*M_{23} + md_{33}*M_{33} + md_{43}*M_{43})*md_{33} + (M_{14} + md_{23}*M_{24} + md_{33}*M_{34} + md_{43}*M_{44})*md_{43}$$

$$NM_{44}=(M_{11} + md_{24}*M_{21} + md_{34}*M_{31} + md_{44}*M_{41}) + (M_{12} + md_{24}*M_{22} + md_{34}*M_{32} + md_{44}*M_{42})*md_{24} + (M_{13} + md_{24}*M_{23} + md_{34}*M_{33} + md_{44}*M_{43})*md_{34} + (M_{14} + md_{24}*M_{24} + md_{34}*M_{34} + md_{44}*M_{44})*md_{44}$$

$$[MODE]^T[K][MODE] = \begin{bmatrix} NK_{11} & 0 & 0 & 0 \\ 0 & NK_{22} & 0 & 0 \\ 0 & 0 & NK_{33} & 0 \\ 0 & 0 & 0 & NK_{44} \end{bmatrix}$$

$$NK_{11}=(K_{11} + md_{21}*K_{21})+ (K_{12}+ md_{21}*K_{22} + md_{31}*K_{32} + md_{41}*K_{42})*md_{21}$$
$$+ (md_{21}*K_{23} + md_{31}*K_{33} + md_{41}*K_{43})*md_{31}$$
$$+ (md_{21}*K_{24} + md_{31}*K_{34} + md_{41}*K_{44})*md_{41}$$

$$NK_{22} =(K_{11}+ md_{22}*K_{21})+ (K_{12} + md_{22}*K_{22}+ md_{32}*K_{32} + md_{42}*K_{42})*md_{22}$$
$$+ (md_{22}*K_{23} + md_{32}*K_{33} + md_{42}*K_{43})*md_{32}$$
$$+ (md_{22}*K_{24} + md_{32}*K_{34} + md_{42}*K_{44})*md_{42}$$

$$NK_{33}= (K_{11}+ md_{23}*K_{21})+ (K_{12}+ md_{23}*K_{22} + md_{33}*K_{32} + md_{43}*K_{42})*md_{23}$$
$$+ (md_{23}*K_{23} + md_{33}*K_{33} + md_{43}*K_{43})*md_{33}$$

$$+ (md_{23}*K_{24} + md_{33}*K_{34} + md_{43}*K_{44})*md_{43}$$

$$NK_{44}=(K_{11}+ md_{24}*K_{21})+ (K_{12} + md_{24}*K_{22} + md_{34}*K_{32} + md_{44}*K_{42})*md_{24}$$
$$+ (md_{24}*K_{23} + md_{34}*K_{33} + md_{44}*K_{43})*md_{34}$$
$$+ (md_{24}*K_{24} + md_{34}*K_{34} + md_{44}*K_{44})*md_{44}$$

$$[MODE]^T*[\ P\ ] = \begin{bmatrix} P_1 + P_2*md_{21} + P_3*md_{31} + P_4*md_{41} \\ P1 + P_2*md_{22} + P_3*md_{32} + P_4*md_{42} \\ P_1 + P_2*md_{23} + P_3*md_{33} + P_4*md_{43} \\ P_1 + P_2*md_{24} + P_3*md_{34} + P_4*md_{44} \end{bmatrix}$$

The equations in independent co-ordinates are

$$NM_{11}*\ddot{U}_1 + (co*NM_{11} + c_1*Nk_{11})*\dot{U}_1 + NK_{11}*U_1$$
$$= P_1 + P_2*md_{21} + P_3*md_{31} + P_4*md_{41} \quad \ldots\ldots\ldots \quad 4.15$$

$$NM_{22}*\ddot{U}_2 + (co*NM_{22} + c_1*Nk_{22})*\dot{U}_2 + NK_{22}*U_2$$

$$= P_1 + P_2*md_{22} + P_3*md_{32} + P_4*md_{42} \quad \ldots\ldots\ldots \quad 4.17$$

$$NM_{33}*\ddot{U}_3 + (co*NM_{33} + c_1*Nk_{33})*\dot{U}_3 + NK_{33}*U_3$$

$$= P_1 + P_2*md_{23} + P_3*md_{33} + P_4*md_{43} \quad \ldots\ldots\ldots \quad 4.18$$

$$NM_{44}*\ddot{U}_4 + (co*NM_{44} + c_1*Nk_{44})*\dot{U}_4 + NK_{44}*U_4$$

$$= P_1 + P_2*md_{24} + P_3*md_{34} + P_4*md_{44} \quad \ldots\ldots\ldots \quad 4.19$$

4.1.8 RESPONSE OF THE END EFFECTOR

Now depending upon whether Z_B is sinusoidal or square the above set of equations can be solved accordingly. Then one can go back to equation 4.4 and get the response in the joint space. As soon as the response in the joint space is known, they can readily be converted to cartesian space to find the end effector response.

One can write,

$$\vec{R_p} = Ex*\hat{i} + Ey*\hat{j} + Ek*\hat{k}$$

Where, $\vec{R_p}$ is the position vector of the end effector with respect to the base co-ordinate frame. Ex, Ey, Ez and $\hat{i}$, $\hat{j}$, $\hat{k}$ are the components and the unit vectors in X_B, Y_B and Z_B directions respectively.

If Exo, Eyo, Ezo are the components corresponding to the equilibrium configuration, it can be written as,

$$E_x - E_{xo} =$$

$$L_5*[S_{1o}*\{\phi_{33}(S_{5o}*C_{3o}*C_{4o} + S_{3o}*C_{5o}) - \phi_{44}*S_{3o}*S_{4o}*S_{5o}$$

$$+ \phi_{55}(S_{3o}*C_{4o}*C_{5o} + S_{5o}*C_{3o})\} + C_{1o}(\phi_{44}*S_{5o}*C_{4o} + \phi_{55}*S_{4o}*C_{5o}]$$

$$+ S_{1o}*[(L_3 + L_4)*\phi_{33}*S_{3o} + \phi_{22}*L_2*S_{2o}] \quad \ldots\ldots\ldots\ldots\ldots\ldots 4.20$$

$$E_y - E_{yo} =$$

$$L_5*[-C_{1o}*\{\phi_{33}(S_{5o}*C_{3o}*C_{4o} + S_{3o}*C_{5o}) - \phi_{44}*S_{3o}*S_{4o}*S_{5o}$$

$$+ \phi_{55}(S_{3o}*C_{4o}*C_{5o} + S_{5o}*C_{3o})\} + S_{1o}(\phi_{44}*S_{5o}*C_{4o} + \phi_{55}*S_{4o}*C_{5o}]$$

$$- C_{1o}*[(L_3 + L_4)*\phi_{33}*S_{3o} + \phi_{22}*L_2*S_{2o}] \quad \ldots\ldots\ldots\ldots\ldots\ldots 4.21$$

$$E_z - E_{zo} =$$

$$L_5*[\phi_{33}(C_{3o}*C_{5o} - S_{3o}*S_{5o}*C_{4o}) - \phi_{44}*S_{4o}*S_{5o}*C_{3o} +$$

$$\phi_{55}(C_{3o}*C_{4o}*C_{5o} - S_{3o}*S_{5o})]$$

$$+[\phi_{22}*L_2*C_{2o} + (L_3 + L_4)*\phi_{33}*C_{3o} + Z_B] \quad \ldots\ldots\ldots\ldots\ldots\ldots 4.22$$

The above equations give the position of the end effector at any time with respect to the equilibrium configuration.

The procedure of finding end effector response of a 5_D.O.F robot when subjected to random excitation is the same as 2_D.O.F system . Hence, to avoid clumsiness,the formulation is not shown. Direct expressions would be used whenever required .

4.2 : SIX D.O.F SYSTEM

If one observes the direction of rotation of the 6^{th} joint, it can be noticed that there is no disturbing couple so that the 6^{th} link can vibrate . Hence the 6^{th} link can be taken as frozen with the 5^{th} link. Any arbitrary amount of rotation of the 6^{th} joint does not change the position of the EE tip. This is because it is axisymmetric and also the last link of the robot. Hence

the contribution of the 6^{th} link to the system KE and PE can be found out without much headache as they are no way functions of ϕ_{66}.

Hence, the only alteration to be made is to replace ${}^{5}I_{yy}$ by ${}^{5}F_{yy}$, ${}^{5}I_{zz}$ by ${}^{5}F_{zz}$, M_5 by (M_5+M_6) and L_5 by (L_5+L_6)

where,

F stands for frozen

and

$$ {}^{5}F_{yy} = M_5*\left(\frac{L_5^2}{3} + \frac{R_5^2}{4}\right) + M_6*\left(\frac{L_6^2}{12} + \frac{R_6^2}{4}\right) + M_6*\left(\frac{L_6}{2} + L_5\right)^2 $$

$$ {}^{5}F_{zz} = M_5*\frac{R_5^2}{2} + M_6*\frac{R_6^2}{2} $$

Now getting the new mass, length and inertia of the 5^{th} link one can follow the same approach as of 5_D.O.F system to find the end effector response for any kind of excitation .

4.3 SUMMARY

This chapter has dealt with the response of the end effector of a five and six D.O.F manipulator for various type of excitations. The frequency equation 4.7 developed will give a basis of the stability of the system when perturbed from the equilibrium configuration. The modal analysis gives an idea of how the different modes take part in vibration. The expressions obtained in this chapter will be used in chapter 5 for numerical calculations and discussions.

CHAPTER 5

NUMERICAL RESULTS AND DISCUSSIONS

5.1 THE INPUT PARAMETERS

In chapter 4, the frequency equation 4.7 and the expressions for response [eqn.4.20-4.22] of the end-effector for different kind of loadings were derived. In order to perform numerical calculations with these equations, one must assign numerical values to the parameters that appear in these equations. These parameters are of two types -

a) System parameters, such as mass, length, radius of the links, rotational stiffnesses of different joints etc.

b) Non-system parameters, such as damping constant, joint angles, external loadings etc.

System parameters are constant for a particular make of robot. The non-system parameters may vary depending upon the configuration of the structure and the environment in which it works. We have considered PUMA_560 as our system. The system parameters are chosen from ref.[16]. These are given in Table 5.1 and 5.2

Selecting values for some of the non-system parameters is not an easy task. If one tries to analyze the system for the actual condition, he has to rely on experimental data, which in many

cases, are derived on the basis of some simplifying assumptions. Joint damping values are difficult to obtain with reasonable accuracy because of its dependence on temperature, nature of lubricant etc.

The author has assumed some value of the damping constants $C_0 = C_4 = 0.01$ but other combination of values can be chosen.

The external loading characteristics may depend on the operating environment. The study is confined to a range of frequencies varying between 10 HZ to 100 HZ, which simulates the base excitation due to a rough surface, undulations in the path of the moving robot, or induced due to ground vibration.

TABLE 5.1

LINK	MASS(k.g.)	LENGTH(mt.)	RADIUS(mt.)
1	12.96		0.17435
2	22.37	0.4318	0.02637
3	5.01	0.37382	0.00648
4	1.18	0.05625	0.0076157
5	0.62	0.05625	0.00424
6	0.16	0.00375	0.007828

The rotational stiffnesses of the joints are as follows:

$K_1 = 3*10^9$ N-M/RADIAN.

$K_2 = 1.8*10^9$ N-M/RADIAN.

$K_3 = 1.0*10^9$ N-M/RADIAN.

$K_4 = K_5 = K_6 = 500$ N-M/RADIAN.

The joint range of the different joints are as follows

TABLE: 5.2

JOINT	JOINT RANGE(DEGREE)
1	-160 TO 160
2	-225 TO 45
3	-45 TO 225
4	-110 TO 170
5	-100 TO 100
6	-266 TO 266

5.2 EFFECT OF JOINT PARAMETER VARIATION ON NATURAL FREQUENCIES

The study of the natural frequency of any system is very important in respect of understanding its behavior in the presence of any external forcing agent . A study has been made for a 6_ D.O.F manipulator to know the variation of the natural frequencies with respect to different parameters. These parameters include the joint stiffness, masses of the links, geometric configuration and the load at the tip. As mass and joint are the constant properties of a system, they are held fixed whereas the configuration & the load at the tip are varied for the purpose of our study. Amongst the different joint parameters , ϕ_{ao} is varied between -135° to 135° at fixed values of ϕ_{ko}, $K \neq 3$. Within these limits the values of the joint parameters are

selected e.g. θ_{10}= 135°, ϕ_{20} = 90°, ϕ_{40}= ϕ_{50}= ϕ_{60} =0°.
The significance of this configuration is that the second link is vertical and others are at horizontal position when ϕ_{30}=0°.

With the given values of the parameters, one can observe that the values of the third and the fourth natural frequencies are so high that their variation does not carry much importance in our study. As for example, ω_3 varies between 330 rad/sec to 310 rad/sec, and ω_4 varies between 650 rad/sec to 600 rad/sec when ϕ_{30} is varied between -135°to 135°. Hence, their study is excluded from the work.

The dependence of ω_1 on ϕ_{30} is shown in Fig.6. It may be observed that ω_1 starts decreasing from -135° to a minimum value at 91° and then from 91° onwards it starts increasing . The second frequency ω_2 at first increases until it reaches a maximum at 0° and thereafter, it decreases to a minimum at ϕ_{30} around 118°.

It may also be observed from Fig.6 that for $\phi_{30} < 0°$ ω_1 increases with increasing load whereas for $\phi_{30} > 0°$, it decreases with increasing load . All the 'P=constant' curves intersect in the neighborhood of ϕ_{30} = 0°. This shows very little dependence of ω_1 on 'P' at this configuration. The reason for this dual behavior in the two regions of ϕ_{30} is as follows.

When ϕ_{30} is increased in the positive region, the effective stiffness of the system decreases with increasing load at the tip whereas in the negative region of ϕ_{30}, the effective

stiffness shows a decline with more load .

In Figure 7 ω_2 vs ϕ_{a0}, the behavior of the different curves at constant 'P' carries the same explanation as above.

Let us now focus attention on the other side of ω_1 v.s ϕ_{a0}. It is notable that with the increase in value in 'P' , the curve dips downward towards the ϕ_{a0} axis when $\phi_{a0} \to 0^\circ$. Hence , it is predictable that for some definite value of 'P', ω_1 would contain zero value by touching the ϕ_{a0} axis tangentially at $\phi_{a0} = 91^\circ = \phi_a^*$. One can say that this frequency branch osculates the ϕ_{a0} axis at this point. The particular value of P and ϕ_a^* are called the CRITICAL DIVERGENCE LOAD and OSCULATION ANGLE for the prescribed values of joint parameters. The significance of osculation is that it indicates the onset of instability in the system.

5.3 : DEPENDENCE OF CRITICAL DIVERGENCE LOAD ON Φ_{a0}

Next, we examine the values of the critical divergence load as function of the equilibrium position of the third link of the manipulator . Given the equilibrium angles of the different joints, one can either solve the frequency equation 4.7 for P, with the condition $\omega = 0$ or by iteration method . Throughout this calculation the values ϕ_{k0} , $k \neq 3$ are held fixed and ϕ_{a0} is varied between $0^\circ$and 180°. The choice of such range for ϕ_{a0} is obvious in the context that for $\phi_{a0} < 0^\circ$, with the increase in load at the tip, ω_1 does not dip downward, instead it increases.

Hence with the increase in load the system will never reach to a critical configuration .

In Fig.8, it can be observed that the critical divergence load decreases when ϕ_{so} varies from 0° to 91° and it increases when $\phi_{so} > 91^{\circ}$. The minimum value of the critical divergence load is 100 kg.and occurs at $\phi_{so}=91^{\circ}$. It increases on either side of $\phi_{so}=91^{\circ}$. Hence for this value of ϕ_{so} ,called osculation angle, the structure assumes the weakest configuration This characteristic is in conformity with Fig.6. The nature of such behavior for a 3_D.O.F system is shown by Anderson [8].

5.4 : RESPONSE OF THE END EFFECTOR

5.4.1 : DETERMINISTIC EXCITATION

A) SINUSOIDAL LOAD

The response plots for sinusoidal loading are shown in fig[9 - 14]. The plots for each D.O.F has been taken at two different forcing frequencies . These are ω_1 = 10 rad/sec. and ω_2 = 100 rad/sec. The nature of the plots at different D.O.F for ω_1 and ω_2 shows the similar trend. This result shows that at higher frequencies there is participation of higher modes in the response.

The other distinctive part of the curves lies in the transient part. At higher frequency, transient part stays for longer time with higher amplitude. But at lower frequency, transient part does not have significant amplitude and dies out faster. For high-speed operation of robot, the analysis of response at higher

frequency is required so that the end effector never crosses the stipulated limit of positional accuracy .

B/ LOAD PULSE

The plots of response vs. square load is given in fig.[15 - 20].The analysis of the end effector response is performed at two different values of forcing frequencies as earlier . Square pulse may be thought of consisting of many sinusoidal waves with different amplitudes and frequencies. If any of these frequencies matches with the system natural frequency, the system will undergo large oscillation . But as the system under consideration is damped and also for the fact the n^{th} harmonic in the square pulse possesses $(1/n)^{th}$ amplitude of the 1^{st} harmonic, the system can be saved of severe damage in such occurrence .

In comparison to the plots taken for sinusoidal input, the response is higher in this case. The steady state solution shows tendency to be of impulse type. This is distinctively visible for the lower frequency curve. The transient part is predominantly prevalent in the case of higher frequency .

5.4.2 RANDOM EXCITATION

In FIG.21, the plot of probability and response for different D.O.F robot subjected to white noise excitation is shown. The spectral density of excitation is taken 0.0001 m^2-sec/rad. The upper bound of frequency is taken to be 500 rad/sec. .

The characteristic of each of the curves is similar i.e with the increase in probability the response increases. The curve is steep near the origin and flat as probability approaches unity. The trend amongst the curves is that, for higher D.O.F, for a particular probability, response decreases. This trend reverses for 6_D.O.F. The 6^{th} link being a frozen link, increases the effective length of the 5^{th} link and so the end effector amplitude of oscillation also increases.

5.5: A FEW RECOMMENDATIONS ON PUMA_560

On the basis of the observations in this chapter, one can make a few recommendations on PUMA_560. These are as follows

1) There are some critical values of P at each joint configuration for which the natural frequency of the system may be zero. The system will diverge and cause failure. Hence the maximum value of the external load P that can be carried by the end effector in a particular configuration should not exceed this critical value of P. To be on the safe side, the maximum load at the end effector must not be fixed above the lowest value of the critical divergence load that occurs at the osculation angle.

2) At higher frequencies, the system response transients are large. So, in order to lessen this, damping in the joints should be increased. This will result in the steady state oscillations with low amplitudes. A special focus on the complex nature of the

system receptance is necessary. At high frequencies, it does not die out but slowly assumes an almost constant value [eqn.3.8]. This is of serious consideration when the system has random excitation. If any random process consists of a wide range of frequency, it will cause large oscillations at the joints and decrease the system performance to an alarming level. In this case, one can either increase the joint stiffnesses or isolate the vibration. Isolation of vibration can be done either at the source or in the robot mounting platform. The increase in joint stiffness will increase the natural frequencies which in turn reduces the transmittance at higher frequencies.

Figure 21 shows that the end effector response for a 6_D.O.F robot is more than a 5_D.O.F robot for the same spectral density. It means that any extension of the link after the 6^{th} link should be done with due consideration as it may exceed the stipulated limit of positional accuracy. This also conforms to the robot design where the linkages are usually made to be more light weight as we reach near the end effector.

CHAPTER 6

CONCLUSION

6.1 SUMMARY OF RESULTS

In this investigation the natural frequencies of vibration, the conditions of stability and the end effector response of a mechanical manipulator with six rigid links have been determined. The links are connected through resilient joints that include restoring moments. The small oscillations of the links with respect to an arbitrary equilibrium configuration have been studied and the values of the critical divergence loads have been calculated as function of the configuration of the manipulator. The response of the end effector for sinusoidal, square and random excitation has been found out at different values of forcing frequencies. A comparison of response has ben made amongst manipulators of three different types when subjected to ergodic and stationary random process. Plots of ω vs. ϕ_{30} reveal that the first natural frequency, ω_1, osculates the ϕ_{30} axis at a critical value of P acting at the tip of the manipulator. This proves to be the critical divergence load. The osculation angle ϕ_{30}^* is the angle at which the critical divergence force is a minimum for a given set of configurations .

At high frequency, when there is the participation of the higher modes in the response of the end effector, the transient response seems to be of considerable importance. Robots which are employed in high-speed operation, requires that the end effector response be dampened out in the quickest possible time.So, the selection of the damping parameters can accordingly be made from fig. .

6.2 SCOPE FOR FUTURE WORK

The present work has the following scopes for future.

1> Instead of cylindrical links, actual shapes of the links can be incorporated.

2> Base excitation due to a variety of forcing functions for various makes of robots need to be investigated.

3> There is a need for experimental determination of the joint damping parameter values to model the robots realistically.

4> Elastic deformations of the flexible arms of the light weight robots should also be investigated as it may contribute to the end effector positioning error.

5> An ideal white noise is not practically feasible. Response characteristics of robots due to random excitation having varying spectral densities need to be studied.

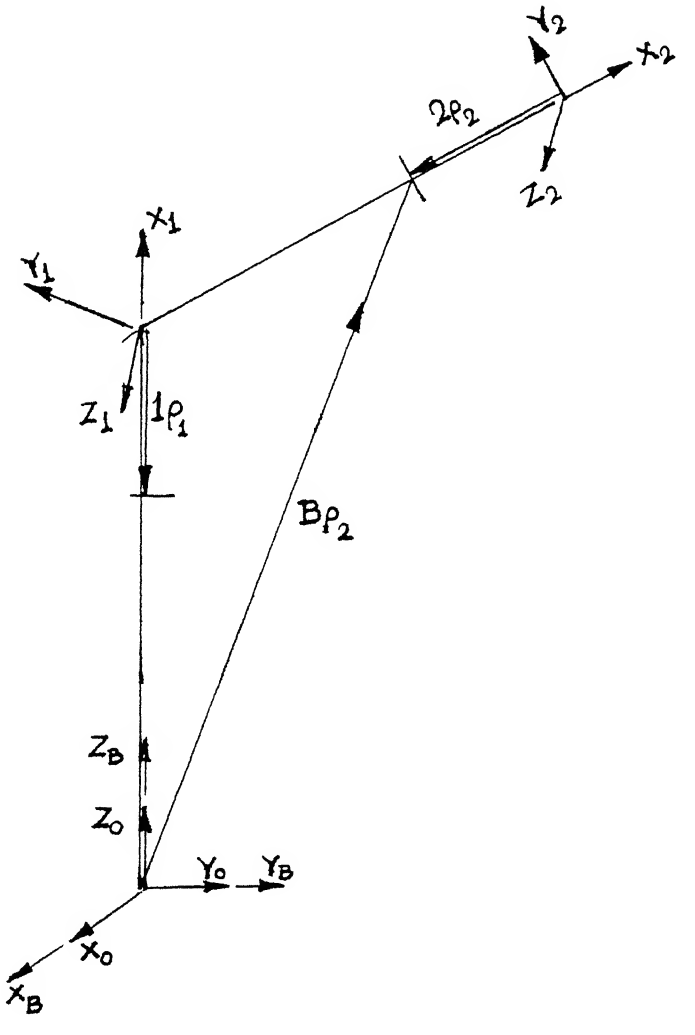

FIG. 3 SCHEMATIC DIAGRAM OF A 2_D.O.F ROBOT.

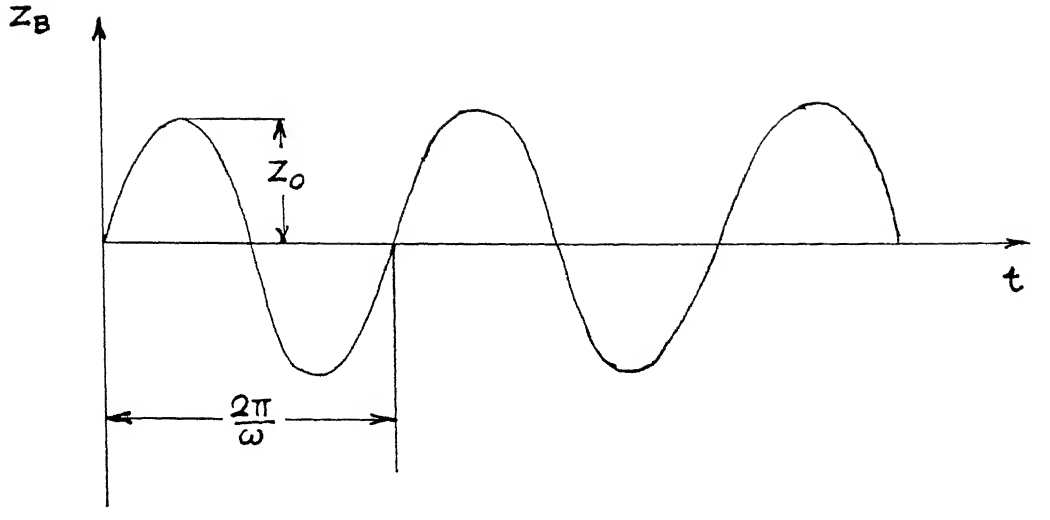

FIG.4 SINUSOIDAL EXCITATION.

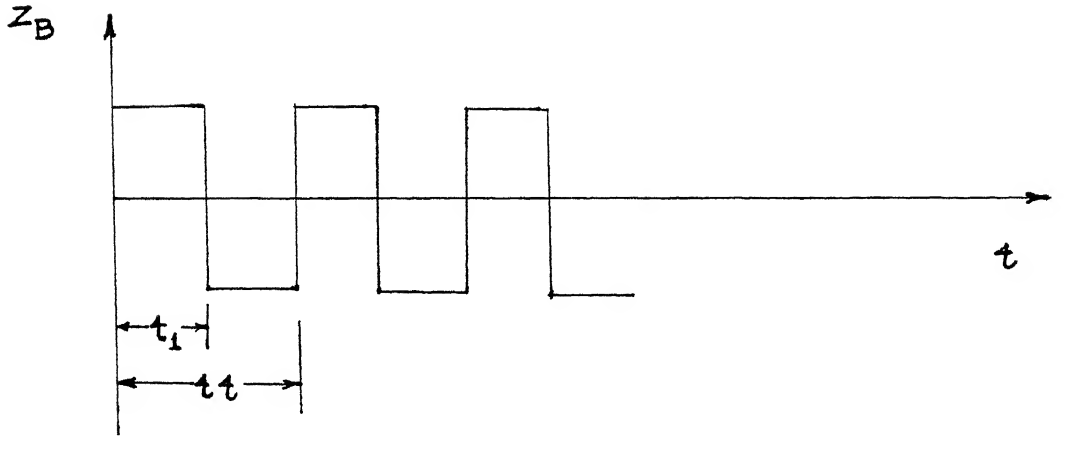

FIG.5 SQUARE PULSE EXCITATION.

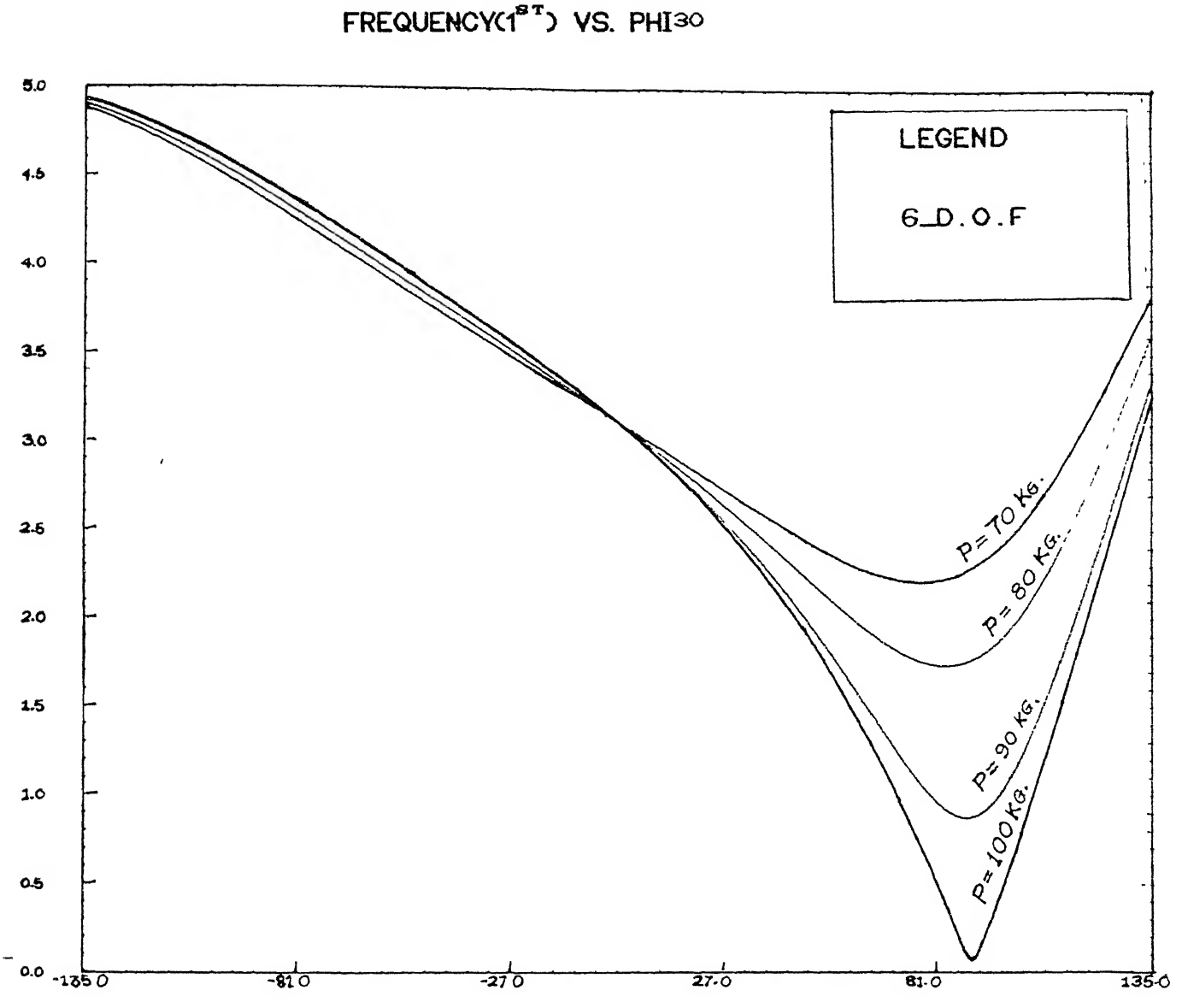
FREQUENCY(1ST) VS. PHI30
LEGEND
6_D.O.F
P=70 KG.
P=80 KG.
P=90 KG.
P=100 KG.
5.0
4.5
4.0
3.5
3.0
2.5
2.0
1.5
1.0
0.5
0.0
-135.0
-81.0
-27.0
27.0
81.0
135.0
φ30(radian)

FIG. 6

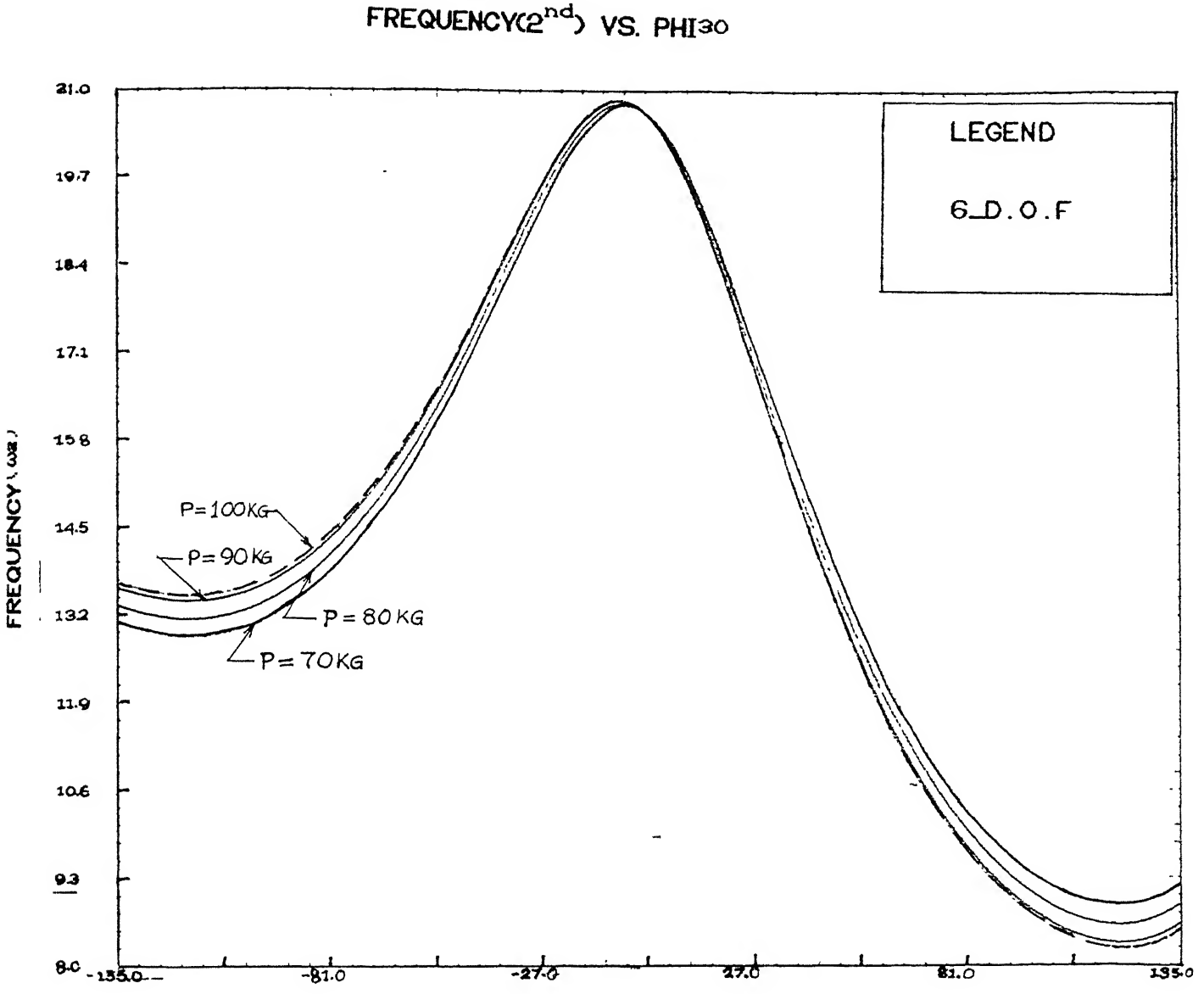
FREQUENCY(2nd) VS. PHI30
LEGEND
6_D.O.F
P=100KG
P=90KG
P=80KG
P=70KG
FREQUENCY
21.0
19.7
18.4
17.1
15.8
14.5
13.2
11.9
10.6
9.3
8.0
-135.0
-81.0
-27.0
27.0
81.0
135.0
φeo(radian)

FIG. 7

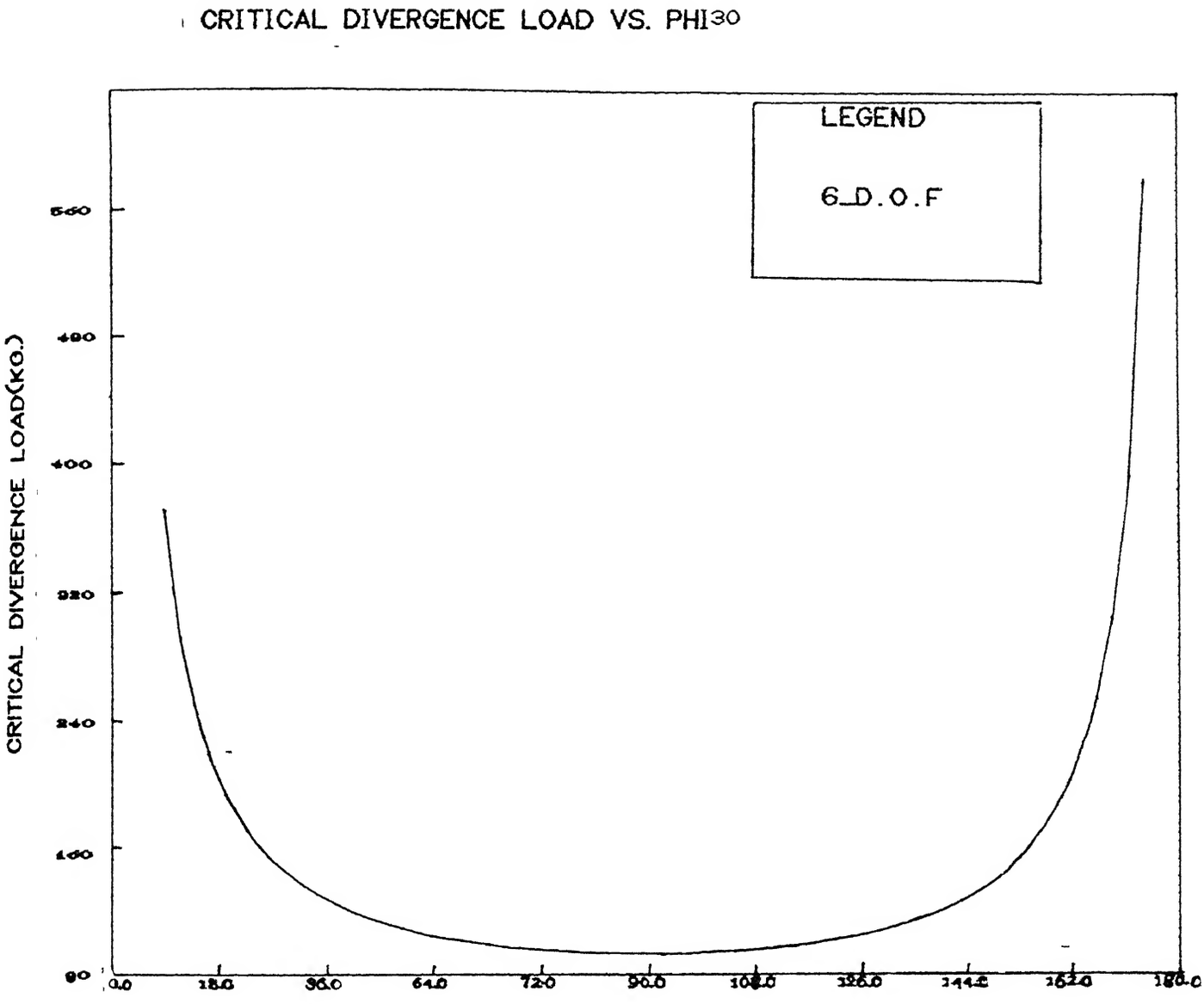
CRITICAL DIVERGENCE LOAD VS. PHI30
LEGEND
6_D.O.F
CRITICAL DIVERGENCE LOAD(KG.)
560
480
400
320
240
160
90
0.0
18.0
36.0
54.0
72.0
90.0
108.0
126.0
144.0
162.0
180.0
φ30(radian)

FIG. 8

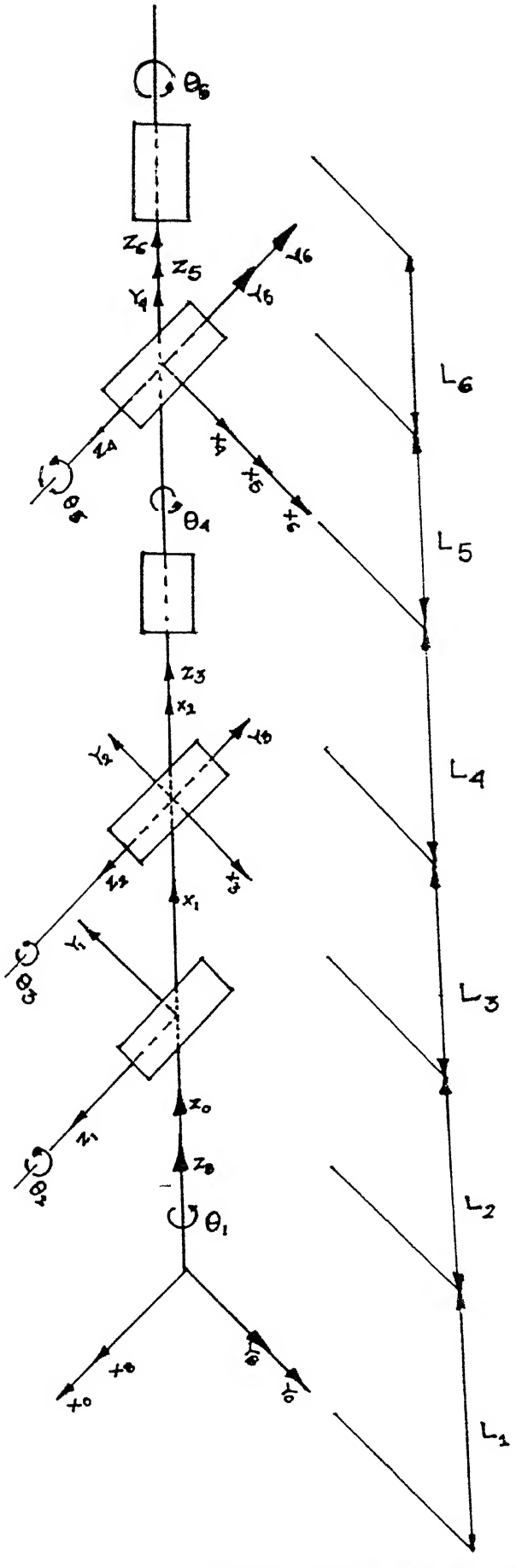

FIG.2 SCHEMATIC DIAGRAM OF PUMA_560.

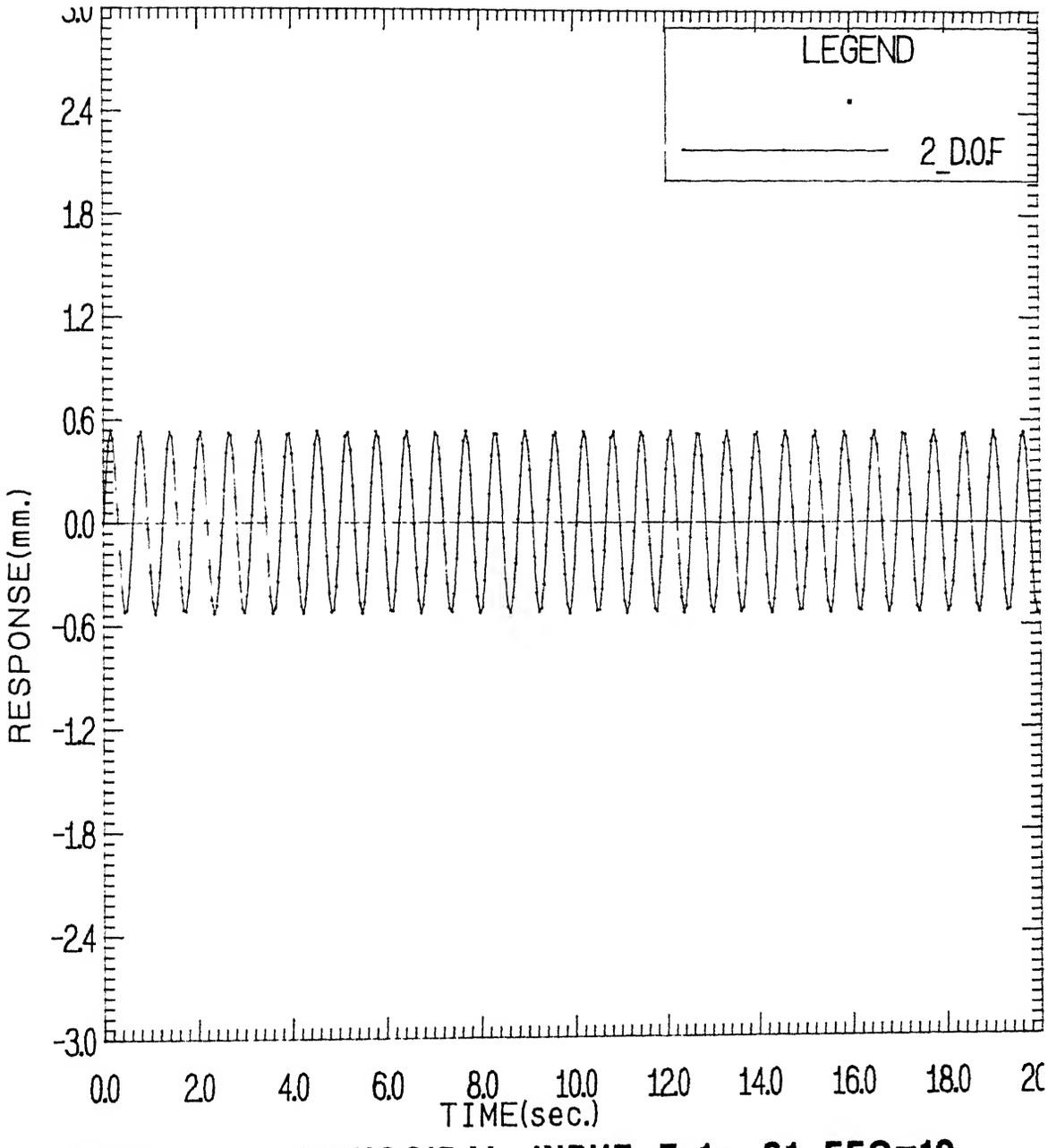

FIG: 9. SINUSOIDAL INPUT Fn1= 31 FFQ=10

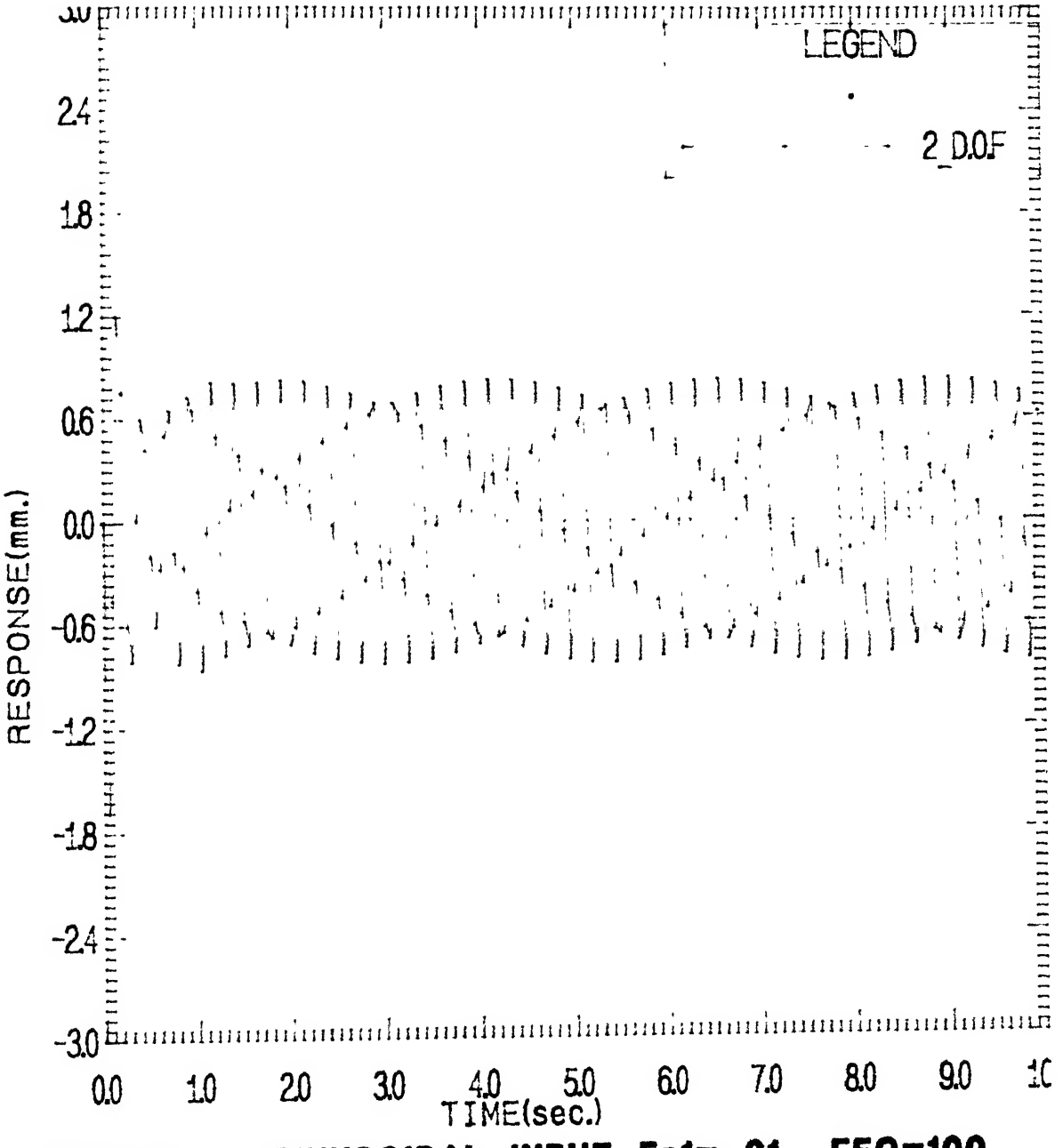

FIG: 10 SINUSOIDAL INPUT Fn1= 31 FFQ=100

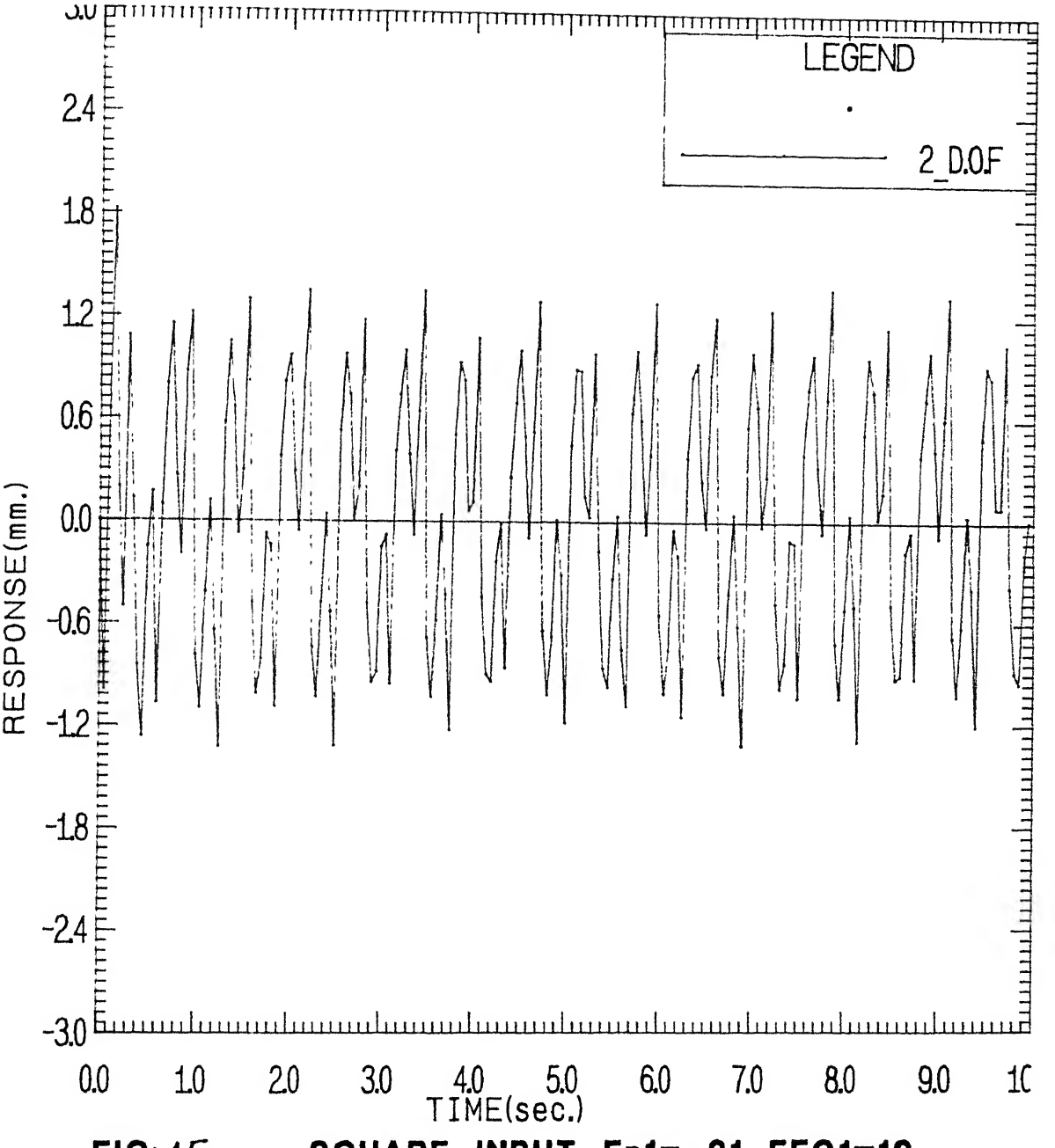

FIG: 15. SQUARE INPUT Fn1= 31 FFQ1=10

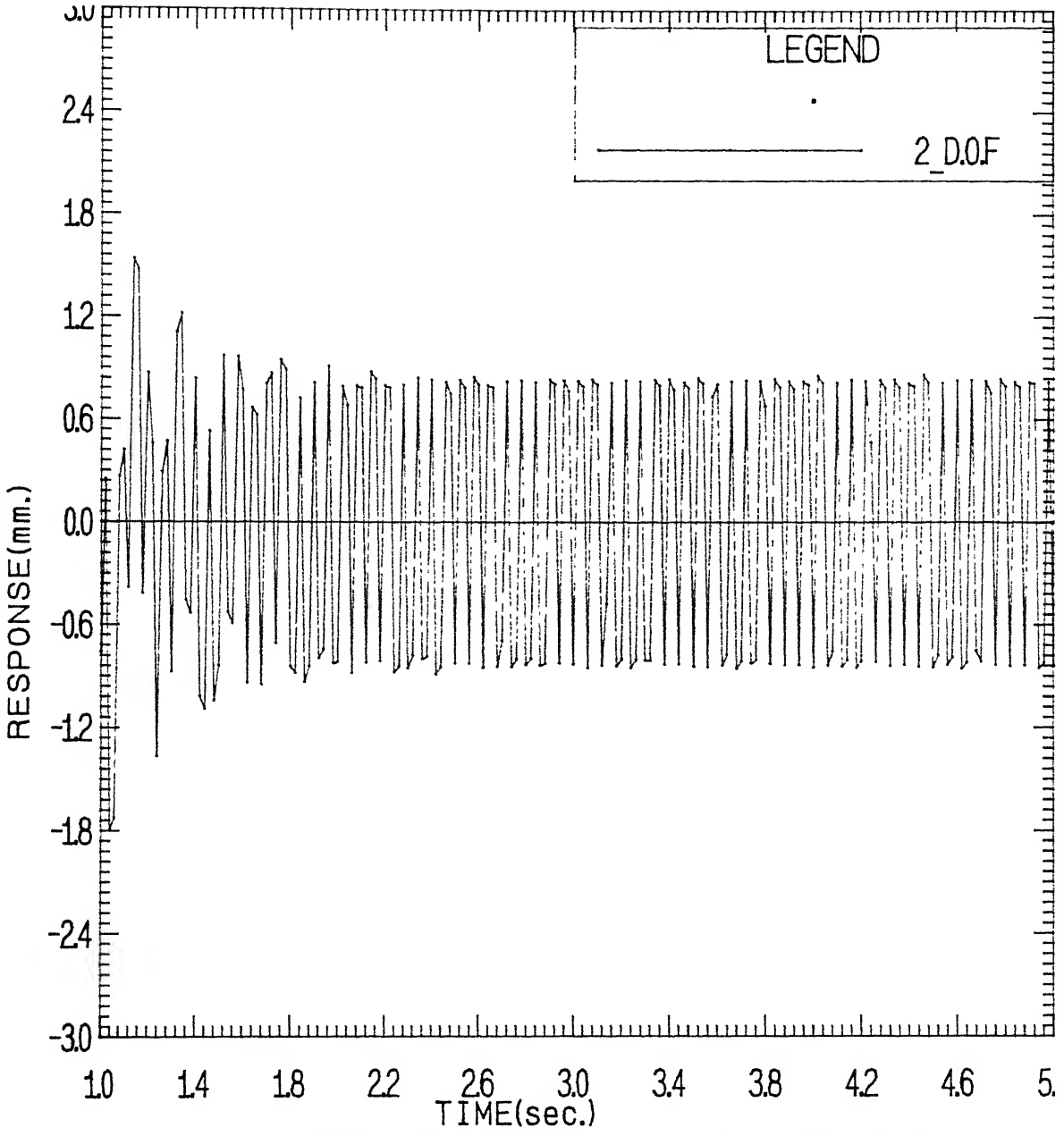

FIG: 16. SQUARE INPUT Fn1= 31 FFQ=100

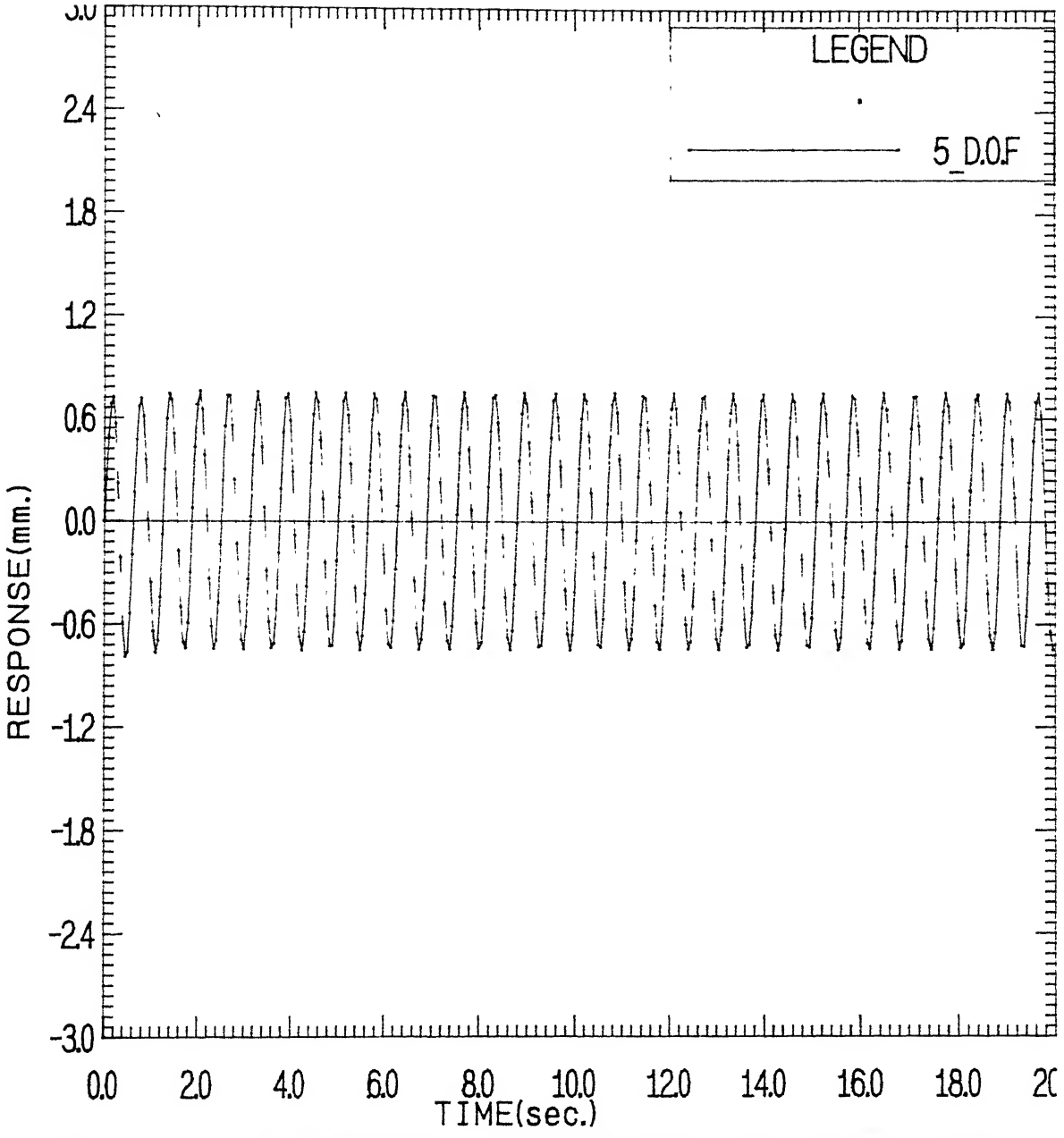

FIG: 11 SINUSOIDAL INPUT Fn1= 18 Fn2= 100 Fn3= 351 Fn4= 800 FFQ=10

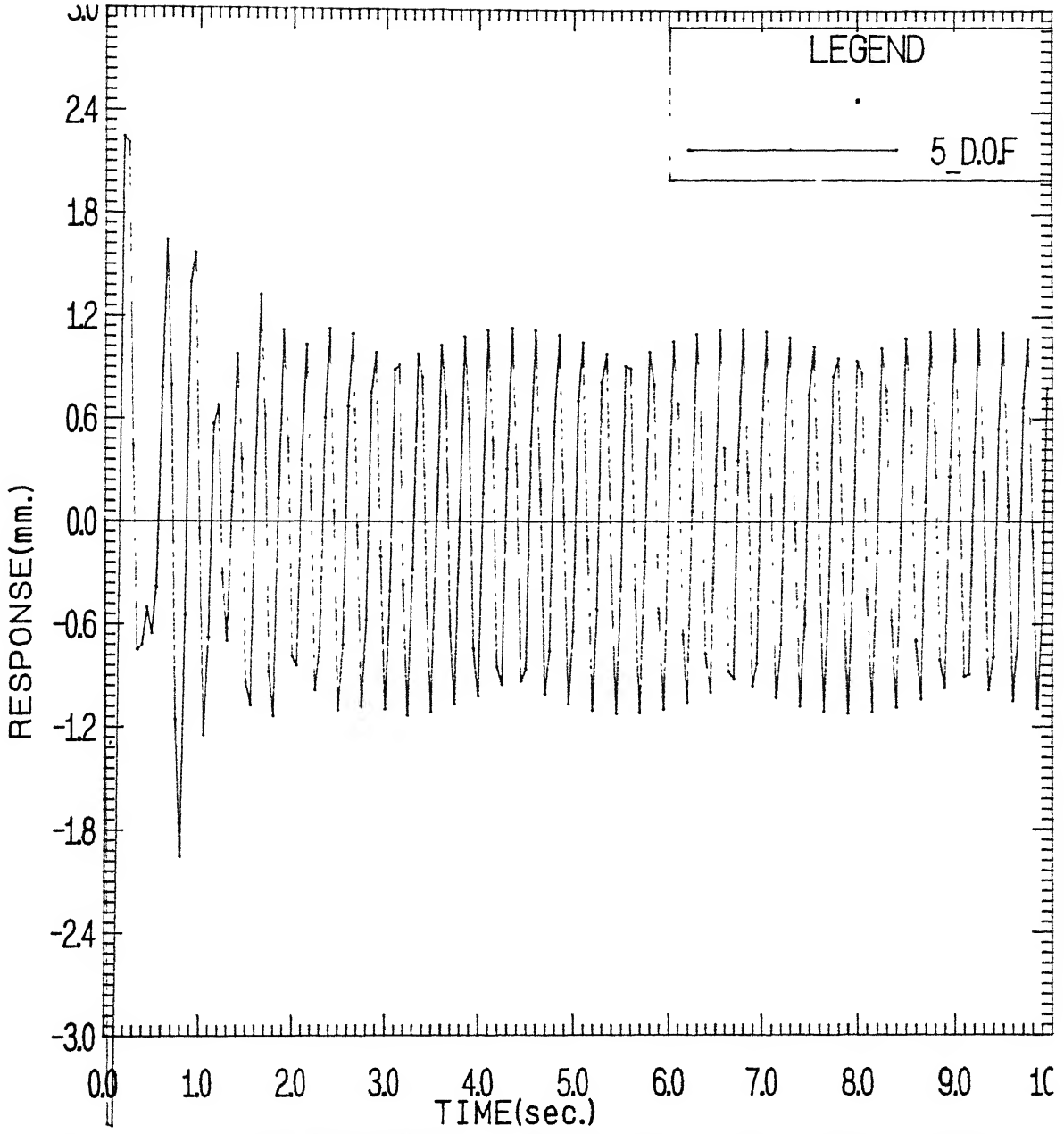

FIG: 12. SINUSOIDAL INPUT Fn1= 18 Fn2= 100 Fn3= 351 Fn4= 800 FFQ=100

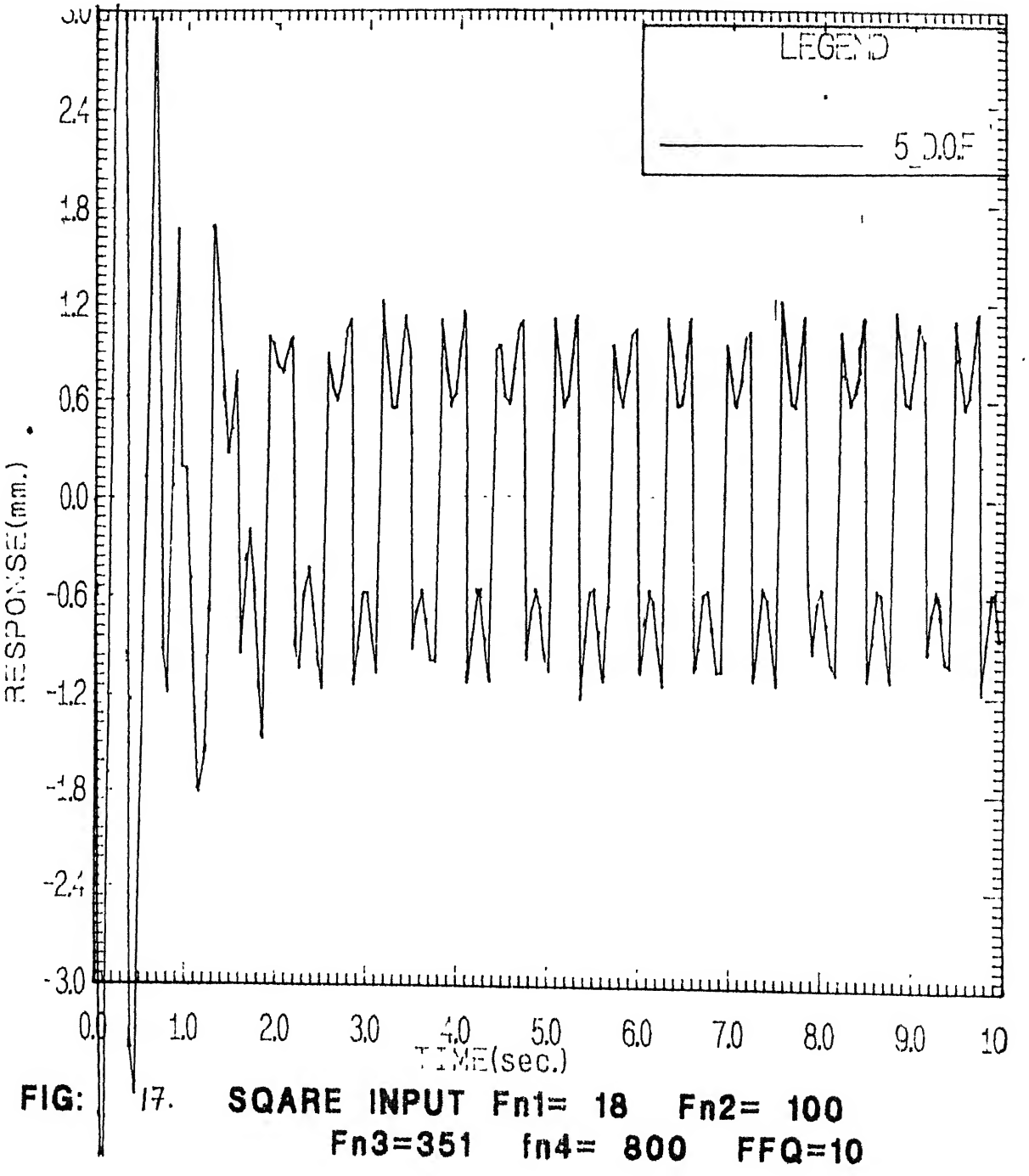

FIG: 17. SQARE INPUT Fn1= 18 Fn2= 100 Fn3=351 fn4= 800 FFQ=10

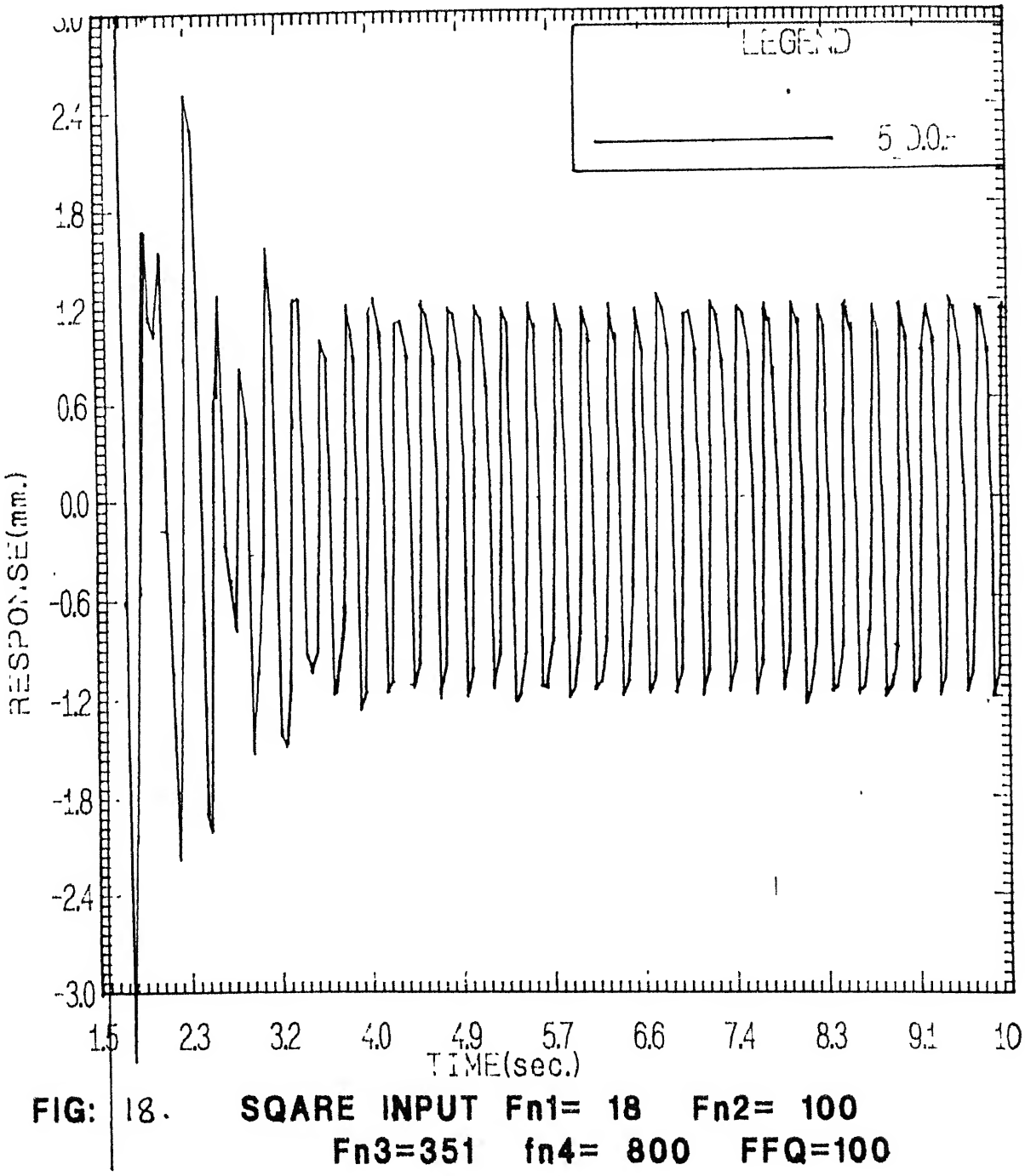

FIG: 18. SQARE INPUT Fn1= 18 Fn2= 100 Fn3=351 fn4= 800 FFQ=100

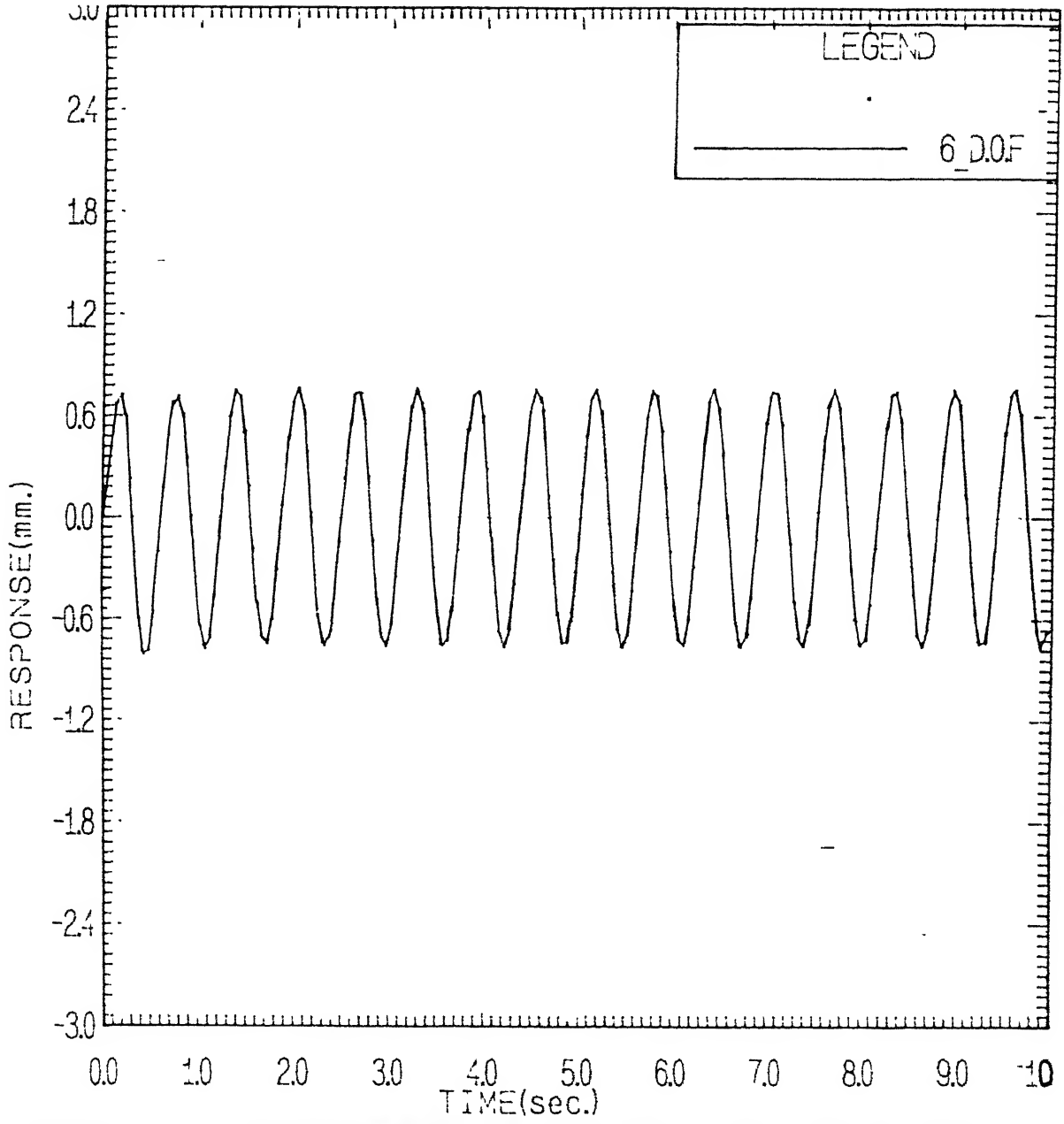

FIG: 13 SINUSOIDAL INPUT Fn1= 18 Fn2= 95 Fn3=343 fn4= 633 FFQ=10

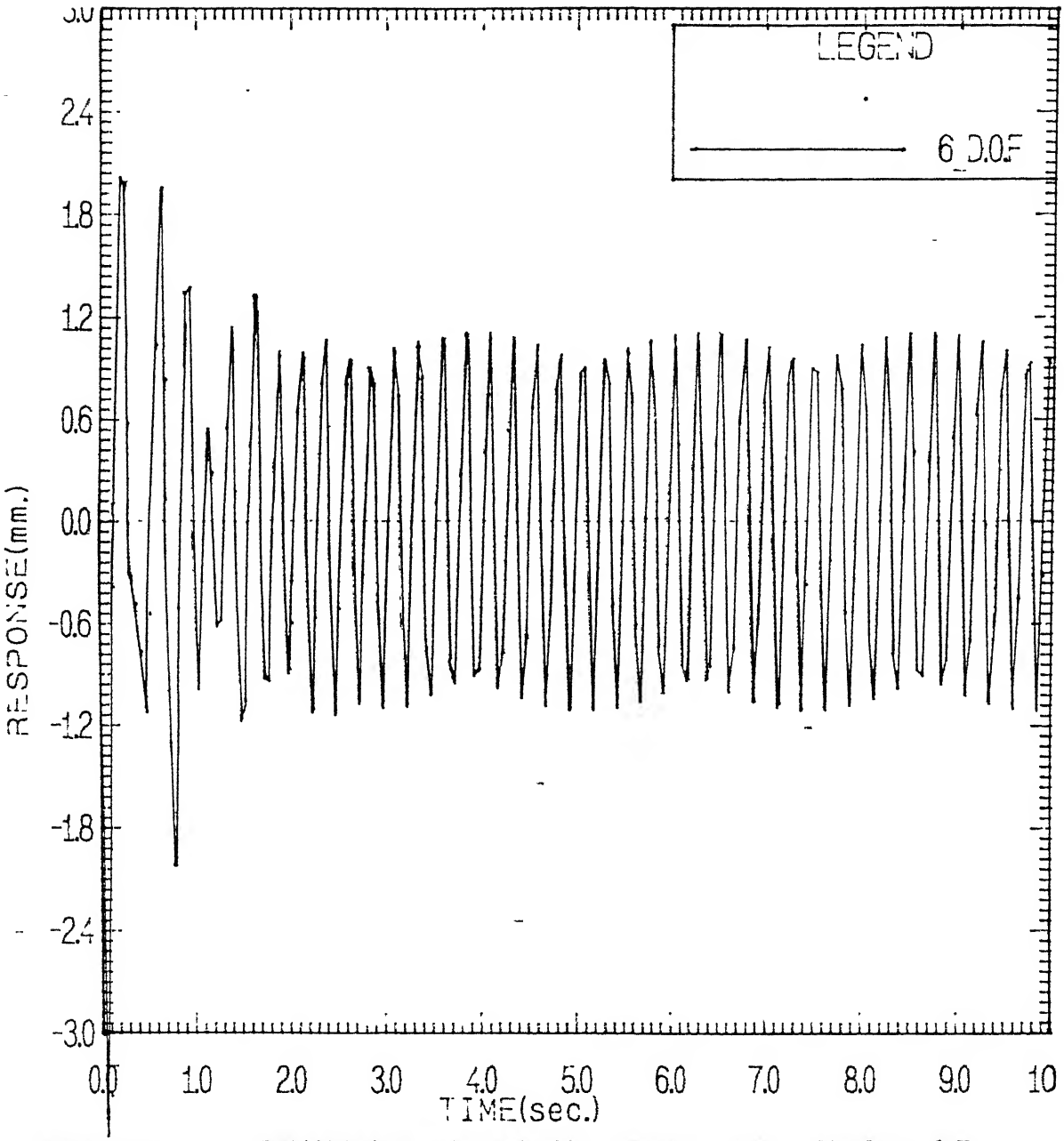

FIG: 14. SINUSOIDAL INPUT Fn1= 18 Fn2= 95 Fn3=343 fn4= 633 FFQ=100

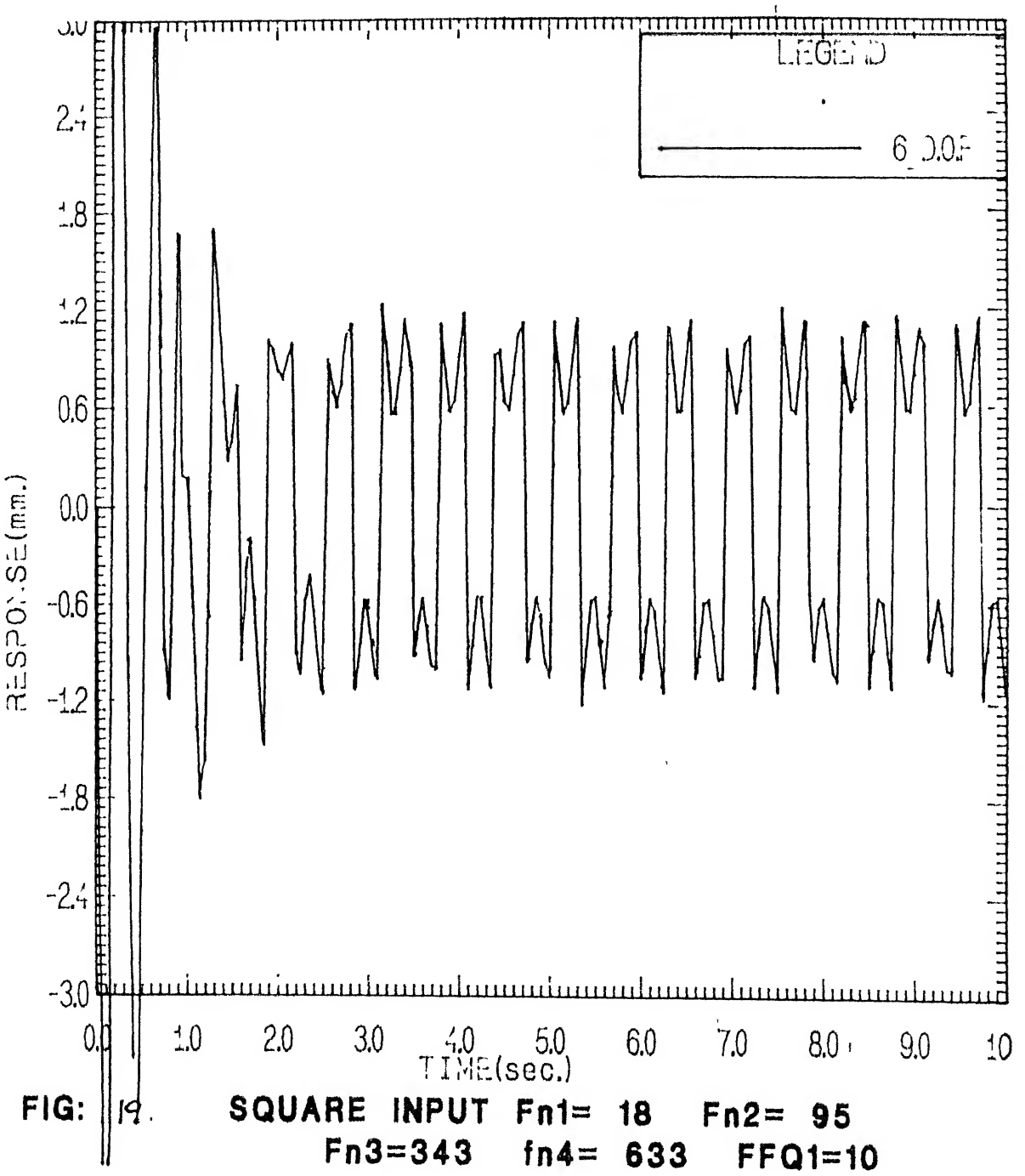

FIG: 19. SQUARE INPUT Fn1= 18 Fn2= 95 Fn3=343 fn4= 633 FFQ1=10

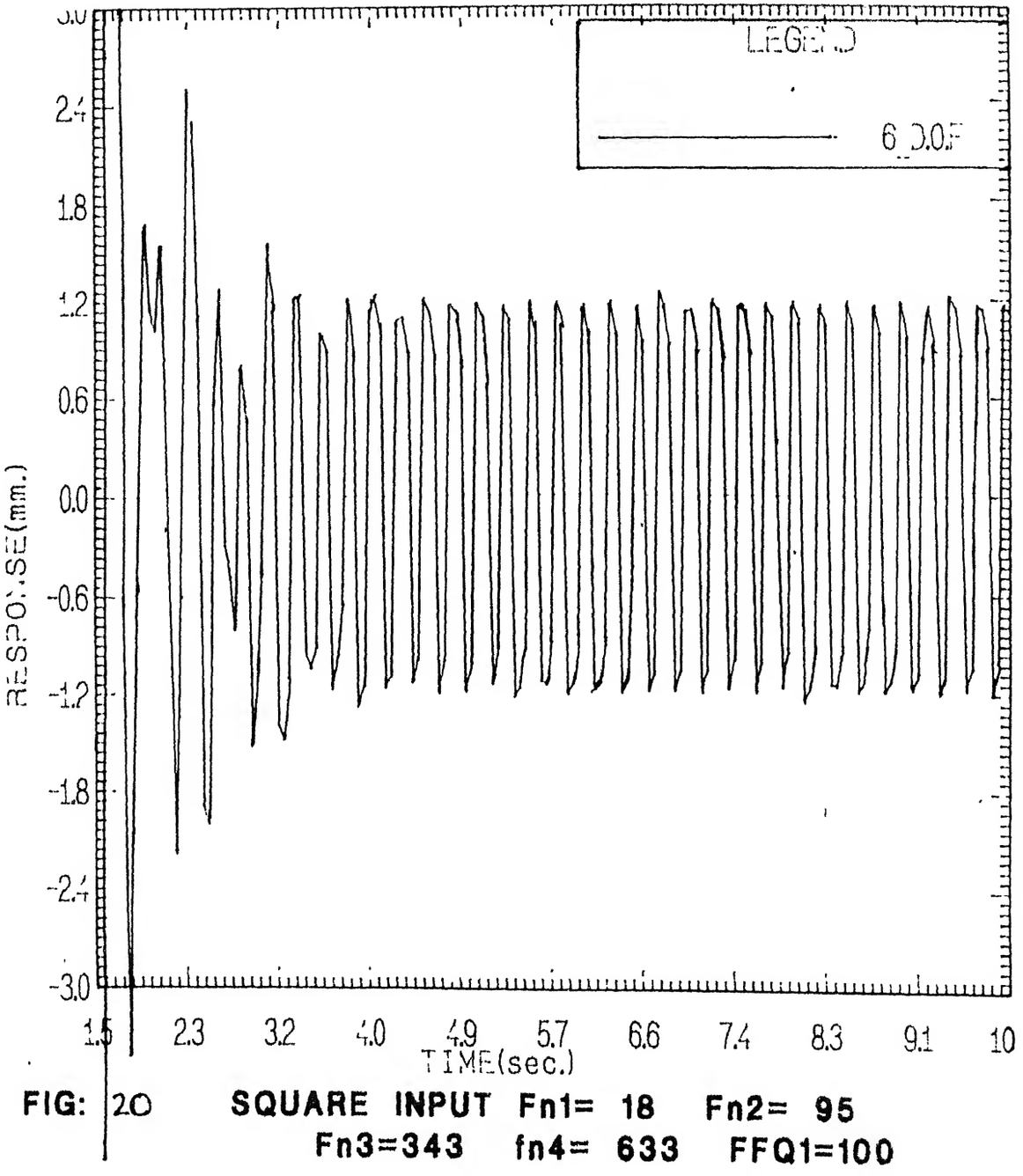

FIG: 20 SQUARE INPUT Fn1= 18 Fn2= 95 Fn3=343 fn4= 633 FFQ1=100

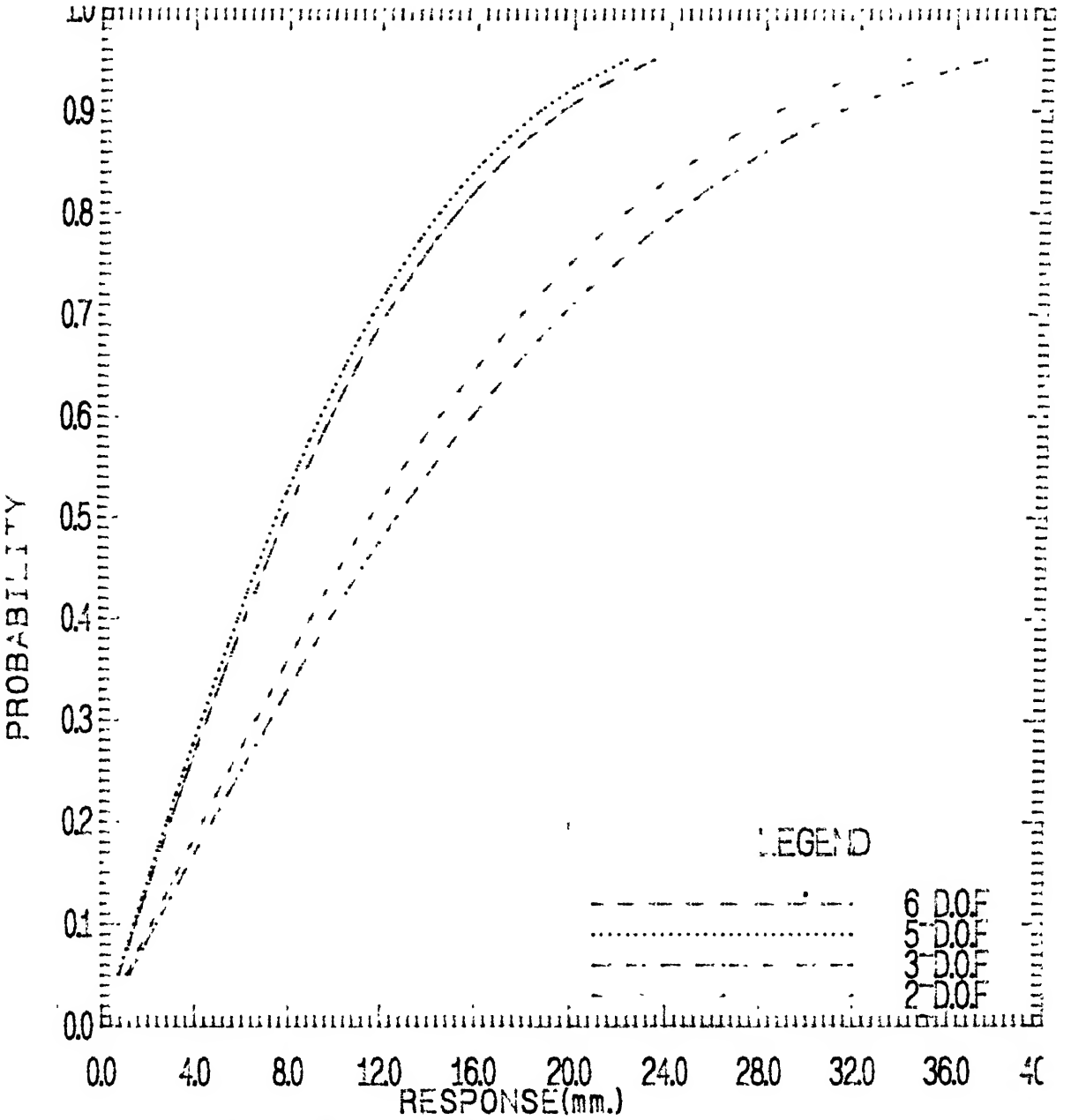

FIG: 21 RANDOM INPUT

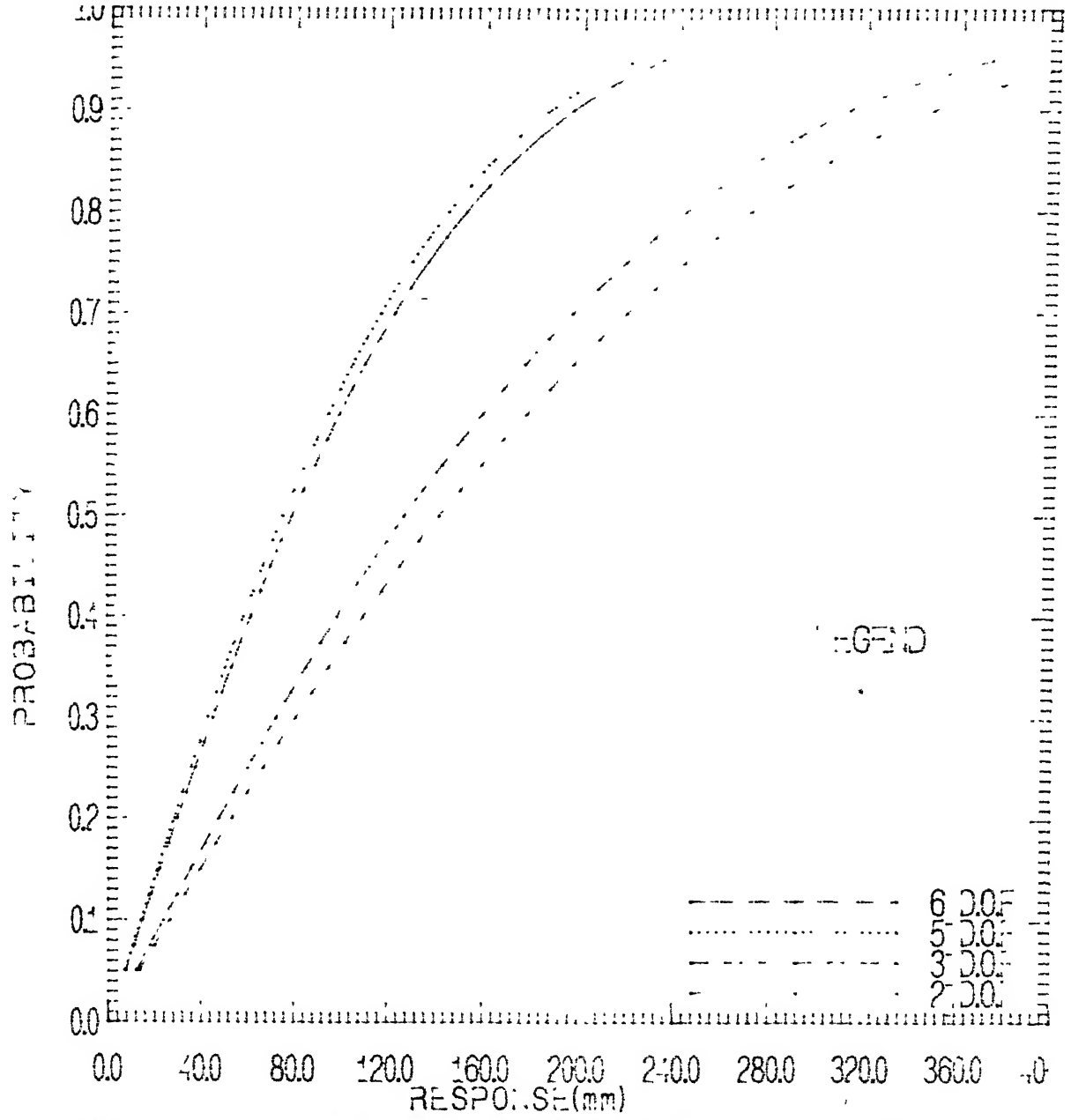

FIG: RANDOM EXCITATION Sp = 0.001

t-iit/k : hpc * 01/31/92 17:50:16 *

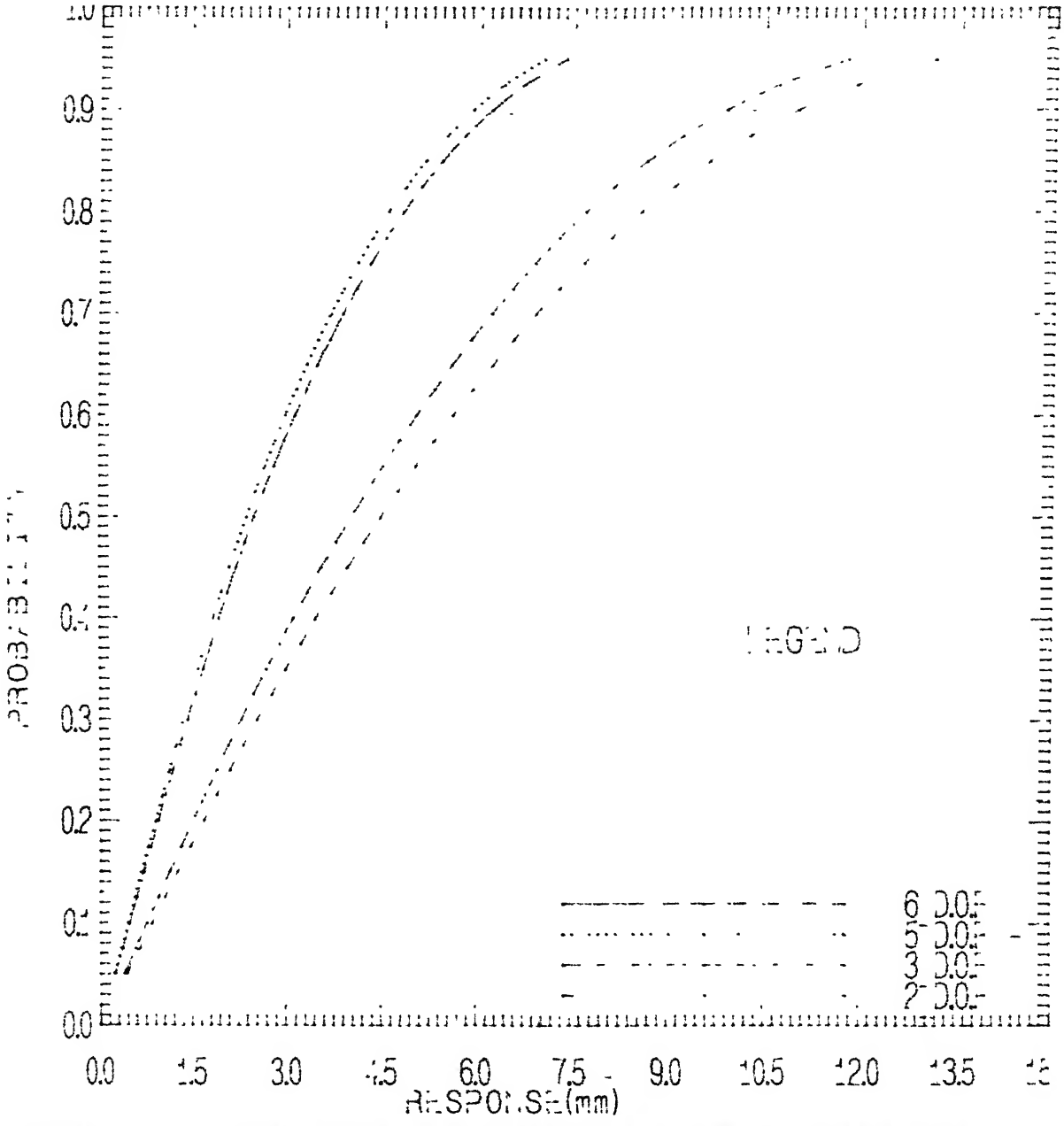

FIG: RANDOM EXCITATION Sp = 0.000001

k : hpc * 01/31/92 17:50:16 *

REFERENCES

1> W. H. Sunada and S. Dubowsky 1982, On the dynamic analysis and behavior of industrial robotic manipulators with elastic members, American Society of Mechanical Engineers, 82-DED-45.

2> P. K. C Wang and Jin Duo Wei 1987, Vibration In Moving Flexible Robot Arm, Journal Of Sound And Vibration(1987) 116(1), 149-160.

3> A. Meghdhari and Shahinpoor 1988, Three Dimensional Flexural-Joint Stiffness Analysis Of Flexible Manipulator Arms, Robotica 6, 203-212

4> S. D. Hill and R. J. Vaccaro 1987, Cartesian Control of Robotic Manipulators With Joint Compliance, Robotica(1987), 5, 207-215.

5> H. Sira-Ramirez and M. W. Spong 1988, Variable Structure Control Of Flexible Joint Manipulators, International Journal Of Robotics And Automation, 3(2).

6> H. Ziegler 1956, On the concept of elastic stability, Advances in applied mechanics, 31, 435-440.

7> G. Herrmann and Bungay 1964, On The Stability Of The Elastic System Subjected To Non-conservative Forces, Journal Of Applied Mechanics 31, 435-440.

8> G. L. Anderson 1985, Stability Of A Manipulator With Resilient Joints, Journal Of Sound And Vibration. 101(4), 463-480.

9> P. K. C Wang and Jin Duo Wei 1987, Feedback Control Of Vibrations In A Moving Flexible Robot Arm With Rotary And Prismatic Joints, Proceedings Of IEEE International

Conference On Robotics And Automation, Raleigh, North Carolina.

10>A J. Critchlow 1985, Introduction To Robotics, Macmillan.

11>K.S.Fu, R.C.Gongalez, C.S.G. Lee 1988, Robotics: Control, Sensing And Intelligence, McGraw-Hill.

12>R.P.Paul 1988, Robot manipulators: Mathematics, Programming And Control, Cambridge, Massachusetts.

13> S.H.Crandall 1958, Random Vibration: Technology Press/Wiley.

14>J.D.Robson 1963, Introduction To Random Vibration, Edinburgh University Press.

15>Y.K.Lin 1967, Probabilistic Theory Of Structural Dynamics, McGraw-Hill.

16>R.C.Dorf 1988, International Encyclopedia of Robotics, 3.

17>R.W.Clough, J.Pengien 1985, Dynamics of Structures, McGraw-Hill.

18> P.G.Ranky and C.Y.Ho 1985, Robot Modelling, IFS Publications.

19>B.S.Grewal 1986, Higher Engineering Mathematics, Khanna publishers.